

100%

90%

80%

70%

60%

50%

40%

30%

20%

10%

0%

0

10

20

30

40

50

60

70

80

90

100

110

120

130

140

150

160

170

180

190

200

210

220

230

240

250

260

270

280

290

300

310

320

330

340

350

360

370

380

390

400

410

420

430

440

450

460

470

480

490

500

510

520

530

540

550

560

570

580

590

600

610

620

630

640

650

660

670

680

690

700

710

720

730

740

750

760

770

780

790

800

810

820

830

840

850

860

870

880

890

900

910

920

930

940

950

960

970

980

990

1000

1010

1020

1030

1040

1050

1060

1070

1080

1090

1100

1110

1120

1130

1140

1150

1160

1170

1180

1190

1200

1210

1220

1230

1240

1250

1260

1270

1280

1290

1300

1310

1320

1330

1340

1350

1360

1370

1380

1390

1400

1410

1420

1430

1440

1450

1460

1470

1480

1490

1500

1510

1520

1530

1540

1550

1560

1570

1580

1590

1600

1610

1620

1630

1640

1650

1660

1670

1680

1690

1700

1710

1720

1730

1740

1750

1760

1770

1780

1790

1800

1810

1820

1830

1840

1850

1860

1870

1880

1890

1900

1910

1920

1930

1940

1950

1960

1970

1980

1990

2000

2010

2020

2030

2040

2050

2060

2070

2080

2090

2100

2110

2120

2130

2140

2150

2160

2170

2180

2190

2200

2210

2220

2230

2240

2250

2260

2270

2280

2290

2300

2310

2320

2330

2340

2350

2360

2370

2380

2390

2400

2410

2420

2430

2440

2450

2460

2470

2480

2490

2500

2510

2520

2530

2540

2550

2560

2570

2580

2590

2600

2610

2620

2630

2640

2650

2660

2670

2680

2690

2700

2710

2720

2730

2740

2750

2760

2770

2780

2790

2800

2810

2820

2830

2840

2850

2860

2870

2880

2890

2900

2910

2920

2930

2940

2950

2960

2970

2980

2990

3000

3010

3020

3030

3040

3050

3060

3070

3080

3090

3100

3110

3120

3130

3140

3150

3160

3170

3180

3190

3200

3210

3220

3230

3240

3250

3260

3270

3280

3290

3300

3310

3320

3330

3340

3350

3360

3370

3380

3390

3400

3410

3420

3430

3440

3450

3460

3470

3480

3490

3500

3510

3520

3530

3540

3550

3560

3570

3580

3590

3600

3610

3620

3630

3640

3650

3660

3670

3680

3690

3700

3710

3720

3730

3740

3750

3760

3770

3780

3790

3800

3810

3820

3830

3840

3850

3860

3870

3880

3890

3900

3910

3920

3930

3940

3950

3960

3970

3980

3990

4000

4010

4020

4030

4040

4050

4060

4070

4080

4090

4100

4110

4120

4130

4140

4150

4160

4170

4180

4190

4200

4210

4220

4230

4240

4250

4260

4270

4280

4290

4300

4310

4320

4330

4340

4350

4360

4370

4380

4390

4400

4410

4420

4430

4440

4450

4460

4470

4480

4490

4500

4510

4520

4530

4540

4550

4560

4570

4580

August 19th 2019

Table of Contents

1 Executive Summary	3
2 Declarations	4
2.1 Relevant Codes and Guidelines.....	4
2.2 Documents Reviewed	4
2.3 Qualifications and Experience	4
2.4 Independence	8
3 Introduction and Scope	8
4. Princess Royal Deposit.....	12
5. Imaging Conductive Structures	15
6. Geodynamic Controls on the Burra Mineral System	17
7. Geochemical Comparison of Burra and Jinchuan	18
7.1 Trace Element Abundances	28
7.1.1 Nickel and Cobalt.....	28
7.1.2 Copper and Cobalt.....	28
7.1.2 Zinc and Copper	30
7.2 CHARAC Ratio Systematics	31
7.2.1 Burra Y/Ho and Zr/Hf Systematics	31
7.3 La/Yb versus Total Rare Earth Projection	34
7.4 Fluid transport of Co and REEs	35
8. Role of Plume Magmatism in Generation of Mineral Deposits	36
8.1 Olympic Dam	36
8.2 Burra Mineral System	37
8.3 Neoproterozoic Mafic Ultramafic Ni-Cu-Co-PGE Deposits in Rodinia....	38
8.4 Exploration Implications for the Burra Project.....	40
9. Summary	43
10. Recommendations	44
11. References	45

1 Executive Summary

This report was commissioned to assess the metallogenic significance of the crustal scale conductivity anomalies identified from magnetotelluric data (AusLAMP survey) at Burra.

Key findings are as follows:

- (1) The multiple conductive regions seen in the MT and AMT images of the lower-to-middle crust at Burra, are interpreted as possible sulphide rich domains.
- (2) Metals in the Burra mineral system were derived from an ultramafic plume source.
- (3) The Burra mineral system formed between ~800 and 830 Ma during the impact of a lower mantle plume below the late Precambrian supercontinent of Rodinia.
- (4) The Jinchuan deposit in China occurs in another dispersed component of Rodinia.
- (5) The Jinchuan deposit is the largest single magmatic sulphide deposit on Earth with >500 Mt @ 1.2% Ni, 0.7% Cu, Cu/Ni 0.58, ~0.4g/t PGE. It formed during the same plume event.
- (6) Jinchuan mineral system was also feed by multiple magmatic conduits.
- (7) Gairdner mafic dykes and samples from Jinchuan were emplaced during the plume magmatic event and have identical lower mantle normalised Ta/U and Nb/Th ratios of ~ unity. This confirms the lower mantle pedigree of their metal sources.
- (8) Princess Royal samples have non-chondritic Y/Ho and both negative and positive Ce/*Ce anomalies. The non-chondritic Y/Ho ratios indicate that the hydrothermal system was halogen-rich (fluorine-rich).
- (9) The negative and positive Ce/*Ce anomalies indicate that the fluids were oxidising.
- (10) Metals at Burra were transported as F-complexes in halogen-rich fluids and as sulphides in pipe-like conduits.
- (11) They were precipitated when fluids interacted with Neoproterozoic carbonate lithologies.
- (12) Willalo rock chip samples display significant coherent enrichment in Co, Cu and Ni. This is interpreted to indicate proximity to the mafic and ultramafic source of metals in the Burra mineral system.
- (13) The primary metal source for Burra mineral system is inferred to be ~300 Ma older than folding in the region associated with the late Precambrian Delamerian Orogeny.
- (14) Mobilisation of mineralisation during this event is likely to have produced zones of sulphide enrichment.
- (15) **This previously unrecognized association Cu-Co-Ni-PGE-Au mineralisation at Burra has a similar source to the giant Jinchuan Deposit in China.**
- (16) An othomagmatic ultramafic source explains this association of metals.
- (17) **Conductive zones A and B west of Princess Royal are likely targets for a Jinchuan type deposit.**
- (18) It is recommended that a gravity survey be undertaken to delineate these conductive zones and to define drilling targets.

2 Declarations

2.1 Relevant Codes and Guidelines

This report has been prepared as a technical assessment in accordance with the "VALMIN Code", as well as the rules and guidelines issued by ASIC and the ASX Limited ("ASX"), which relate to independent Expert Reports (Regulatory Guides RG 111 and RG 112). Where and if mineral resources have been referred to in this Report, the classifications are consistent with the Australasian Code for Reporting of Exploration Results, Mineral Resources and Ore Reserves ("JORC Code"), prepared by the Joint Ore Reserves Committee of the AusIMM in December 2012.

Under the definition provided by the ASX and in the VALMIN Code, these properties under review are classified as "exploration projects". Thus they are potentially speculative in nature. Nevertheless, the properties are considered to be sufficiently prospective to warrant further exploration and development of their economic potential, consistent with the exploration and development programs envisaged by Ausmex Mining Group.

The quoted results are drawn from published and unpublished information and are considered reliable for the purposes of this report.

KDC Consulting was engaged by the Ausmex Mining Group to report on the significance of two shallow conductive structures below the Princess Royal Mine at Burra recently identified using MT, AMT, regional magnetics and gravity.

This Independent Report is not a valuation report and does not express an opinion on the value of the mineral assets or tenements involved, or to the fairness or reasonableness of any transaction involving the property between Ausmex Mining Group and any other party.

2.2 Documents Reviewed

Data reviewed were provided by Ausmex Mining Group Ltd.. Published scientific papers relevant to the review, were identified following a literature search using the "Web of Science" at the University of Queensland.

2.3 Qualifications and Experience

The Author of this report Emeritus Professor Kenneth D. Collerson B.Sc (Hons), Ph.D. FAusIMM has over 48 years of experience as a professional geologist

This certificate applies to this technical report titled:

"Geological Constraints on the Interpretation of Shallow Conductive Targets Identified by Magnetotellurics at Burra, SA"

that has an effective date of 19th August, 2019.

I am a Fellow of the Australasian Institute of Mining and Metallurgy (#100125). I graduated in 1993 as Doctor of Philosophy (Geology) from the University of Adelaide, South Australia and also have a Bachelor of Science degree with 1st Class Honours from University of New England, N.S.W., Australia (awarded in 1997). Emeritus Professorial status at the University of Queensland acknowledges my contribution to research, management and teaching in the University sector.

I have practiced my profession as a Principal Consultant with Salva Resources, HDR Salva and Caracle Creek (Toronto) and as a self-employed consultant for more than 35 years. As a Principal Consultant in mineral exploration I have an excellent record of discovery. I have worked on a variety of multi-commodity metals exploration projects through high-level consulting activities in more than 15 countries.

In a consultancy for Geological Survey of Queensland (2014-2016) using spinifex grass as a biogeochemical exploration medium in the Simpson Desert, in 2014 I discovered a Devonian age alkaline metallogenic province, (Diamantina Province). Importantly, I showed that the Diamantina Province is part of a much larger belt (a plume track) of ~ 440 Ma to 365 Ma igneous activity that extends more than 2000 km from central NSW to the Northern Territory. The entire belt is prospective for a range of metals including scandium, cobalt, PGEs, copper, and gold, as well as for diamond.

Recent industry and Government consultancies include:

- Transition Resources Ltd. July 2019 - Mineral System Characterisation and Prospectivity Review of Transition Resources West and East EPMs: Cloncurry District, Queensland.
- Ausmex Ltd. June 2019 - Lithological and Chemical Constraints on the Mount Freda-Evening Star Mineral System, Cloncurry District Improve IOCG Metal Source Targetting
- Queensland DNRM December 2018 - Cobalt and HREE Mineral Systems in the Mount Isa Block
- Impact Minerals Ltd., March 2019 - Neoproterozoic Cu-Co-Ni-Au-PGE Alkaline Mineral System in the Broken Hill District: Lithogeochemical and geodynamic implications for prospectivity.
- Hammer Metals Ltd., October 2018 - Lithogeochemistry of Cu-Co-Ni-Au-PGE-REE mineralisation in the Mary Kathleen Belt: A Mineral System Approach to improve exploration.
- Ausmex Ltd September 2018 - Rare Earth Element - Cobalt-Copper-Gold Mineral System at Burra, S.A: Significance of the AusLAMP Magnetotelluric Anomaly
- Hammer Metals August 2018 - U-Pb Titanite Geochronological Constraints on Origin and Age of the Mount Philip Breccia
- Northern Cobalt June 2018 - Review of Wollongorang Project Chemistry: Mineral System and Exploration Vectors.
- Longford Resources Feb. 2018 - present. Targetting Co and PGE mineralisation in the Goodsprings area, Nevada.
- Hammer Metals Feb. 2018 - Lithological and geochemical interpretation of selected cores from Elaine Dorothy, Blue Caesar and Koppany Prospects.
- Encounter Resources May 2017 - present. Spinifex biogeochemistry proof of concept survey over gold and Co anomalies in the Telfer area, WA

- Laconia Resources Ltd May 2017 - present. Au-Ni-PGE target generation in the Kraaipan Greenstone Belt, Botswana
- Caracle Creek International 2016 - present. Associate Pegmatite Specialist Providing field geological, petrological and geochemical advice for international clients on exploration for LCT pegmatites
- Tyranna Resources June 2016 - present. Improved understanding of calcrete gold geochemistry in the western Gawler Craton that allowed discrimination between true and false calcrete Au anomalies with great success.
- Macarthur Lithium 2016. Provided field geological, petrological and geochemical advice to the MD on lithium exploration in the Pilbara and Yilgarn Cratons. Developed a technique using trace elements in K-feldspar to identify the Li content of the source pegmatite. This IP has global application.
- Impact Minerals Ltd 2015 - present. Petrology and geochemistry of outcrop and drill core samples from Red Hill and Mulga Springs-Moorkaie Intrusions at Broken Hill. Decoded the geochemistry and petrology of PGE-Au-Cu-Ni-Zn mineralisation at Broken Hill, resulting in enhanced understanding of the entire mineral system at Broken Hill, one of Earth's largest accumulations of metals.
- Providence Natural Resources 2012 - present. LCT pegmatite exploration for lithium at Järkvissle in Central Sweden. Currently contracted to find a JV Partner for a JORC Li resource.
- Exco/Copper Chem 2014. Preparation of a geological briefing paper for the Mary Kathleen rare earth Government tender bid.
- Exco 2014. Preparation of a prospectivity assessment for the White Dam area, South Australia, specifically identifying geochemical vectors that allowed improved understanding of the style of mineralisation.
- Chinalco Yunnan Copper Resources Limited 2013 - April 2014. Reviewed and reinterpreted drill core at Elaine and Blue Caesar and developed new model for Cu-Au-Co-REE-U mineralisation in the Mary Kathleen Belt, NW Queensland. I identified the alkaline igneous source of metals in the terrane and demonstrated that these ~1526 Ma alkaline intrusions were emplaced at a shallow crustal depth and produced epithermal mineralisation. As well as improving knowledge of Mary Kathleen Belt mineral systems, this discovery also explains Cloncurry Belt IOCG mineralisation.
- Viti Mining Pty Ltd. 2013 April - Present. Confirmed the existence of world-class very high-grade Mn mineralisation (DSO) at a number of locations on Viti Levu, Fiji. Showed that mineralisation was hydrothermal and occurred as part of an epithermal alteration system above Au-Ag-Cu bearing shoshonite intrusions
- Golden Island Resources Pty Ltd. 2013 April - Present. Undertook a literature review and discovered "lost" reports showing very widely distributed high grade Au and Ag assays (up to 35 g/t) on Waya and Wayasewa. Showed that these islands formed an extension of the shoshonite – gold trend west of Viti Levu, and following recovery of excellent panned concentrate results the islands are now being investigated using soil geochemistry to delineate drill targets.
- Golden Island Resources Pty Ltd. 2013 April - Present. I reprocessed magnetic and gravity data for Viti Levu and discovered a previously unknown ~40 km diameter Au-bearing shoshonite caldera south of Tavua caldera that has never been drilled. The Tavua caldera is host for the >1MOz epithermal Au-Ag Emperor goldmine on Viti Levu.

- Waratah Resources 2012 December. Prospectivity assessment of Gabon and the Republic of the Congo. Reviewed the geochemistry of BIFs in Waratah Resources tenements in Gabon and the Republic of the Congo to facilitate regional exploration and resource estimation.
- ASERA Iron Project 2012. December Geochemical evaluation of Lake Vättern orthomagmatic Fe-Ti-V project, Southern Sweden. Concluded that mineralisation is hosted by an anorogenic anorthosite intrusion not IOCG as previously believed.
- Triton Gold 2012 – August to December. Geochemical interpretation, Au and Mn target assessment on Viti Levu.
- Pacific Wildcat Resources 2011 – July to October. Fieldwork in Kenya and interpretation of DD core from Mrima Hill carbonatite and outcrops of nepheline syenite in a nearby intrusion. Showed that carbonatites and syenites were genetically related forming part of a >10 km diameter intrusion. Discovered an untested mineral system and identified zones of rare earth mineralisation for a subsequent RC and DD drilling program.

I am responsible for all sections of this draft report and am independent of the Mayur as is described by Section 1.5 of NI 43-101. I am confident that this report has been prepared in compliance with the JORC 2012 Code and with the instrument NI 43-101.

As of the effective date of the technical report, to the best of my knowledge, information and interpretation in the report contains all scientific and technical details that are required to be disclosed.

Dated 19th August 2019



Professor Kenneth D. Collerson
Ph.D., FAusIMM
KDC Consulting
33 Cramond St
Wilston, Qld 4051
MOB 0412049602
kencollerson@gmail.com

Forward Looking Statements

The materials may include forward looking statements. Forward looking statements inherently involve subjective judgement, and analysis and are subject to significant uncertainties, risks, and contingencies, many of which are outside the control of, and may be unknown to, the company.

Actual results and developments may vary materially from that expressed in these materials. The types of uncertainties which are relevant to the company may include, but are not limited to, commodity prices, political uncertainty, changes to the regulatory framework which applies to the business of the company and general economic conditions. Given these uncertainties, readers are cautioned not to place undue reliance on forward looking statements.

Any forward-looking statements in these materials speak only at the date of issue. Subject to any continuing obligations under applicable law or relevant stock exchange listing rules, the company does not undertake any obligation to publicly update or revise any of the forward-

looking statements, changes in events, conditions or circumstances on which any statement is based.

Competent Person Statement

Statements contained in this report relating to exploration results and potential are based on information compiled by Professor Ken Collerson, who is a Fellow of the Australasian Institute of Mining and Metallurgy (AusIMM). Professor Ken Collerson is an independent consultant to Ausmex Mining Group Limited and Geologist whom has sufficient relevant experience in relation to the mineralization styles being reported on to qualify as a Competent Person as defined in the Australian Code for Reporting of Identified Mineral resources and Ore reserves (JORC Code 2012). Professor Ken Collerson consents to the use of this information in this report in the form and context in which it appears.

2.4 Independence

I am not, nor intend to be a director, officer or other direct employee of Ausmex Mining Group Ltd., and have no material interest in this project. The relationship with the Company is one of professional association between client and independent consultant. The review work and this Report are prepared in return for professional fees based upon agreed commercial rates and the payment of these fees is in no way contingent on the results of this Report.

3 Introduction and Scope

Understanding geochemical and geodynamic constraints on metal sources, transport mechanisms and depositional environments is critical knowledge to enhance exploration success, particularly when exploring for deep IOCG or Cu-Au porphyry targets (Richards and Mumin 2013).

KDC Consulting was engaged by the Ausmex Mining Group to report on the significance of two shallow conductive structures below the Princess Royal Mine at Burra that were identified using MT, AMT, regional magnetics and gravity (ASX Announcements on August 7 and 14, 2019).

These conductive structures, Targets A and B are shown in Figures 1 and 2.

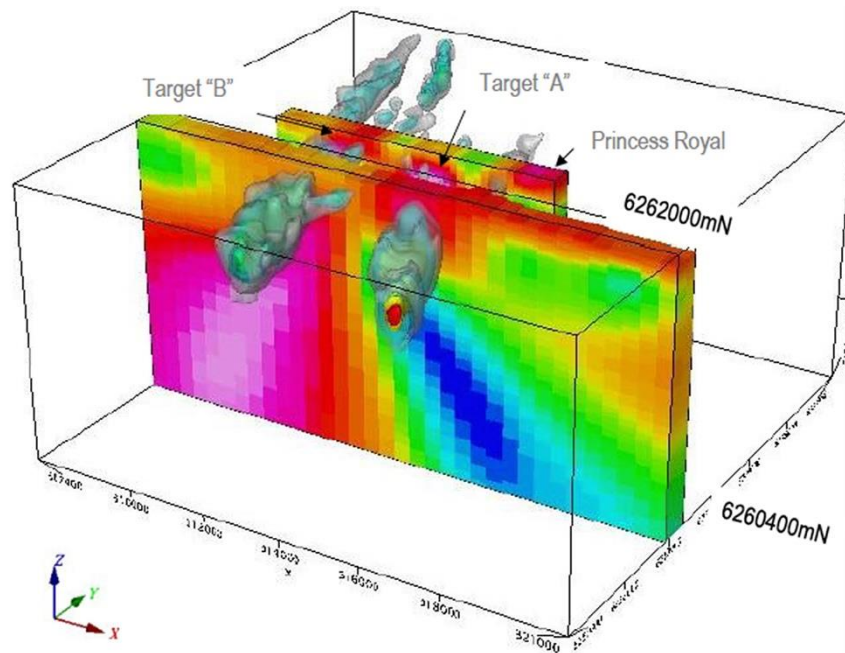


Figure 1: 3D Model viewed to the NW showing targets A and B in relation to Princess Royal Deposit. Targets A and B are seen as large magnetic trends that coincide with a strongly conductive MT/AMT zone that extends to depth. Target A is several km in strike length and extends from near surface to ~1.7 km.

A similar conductive structure that also follows a magnetic anomaly also extends to below the Princess Royal Mine and may be related to the Target A conductive structure (Figure 2).

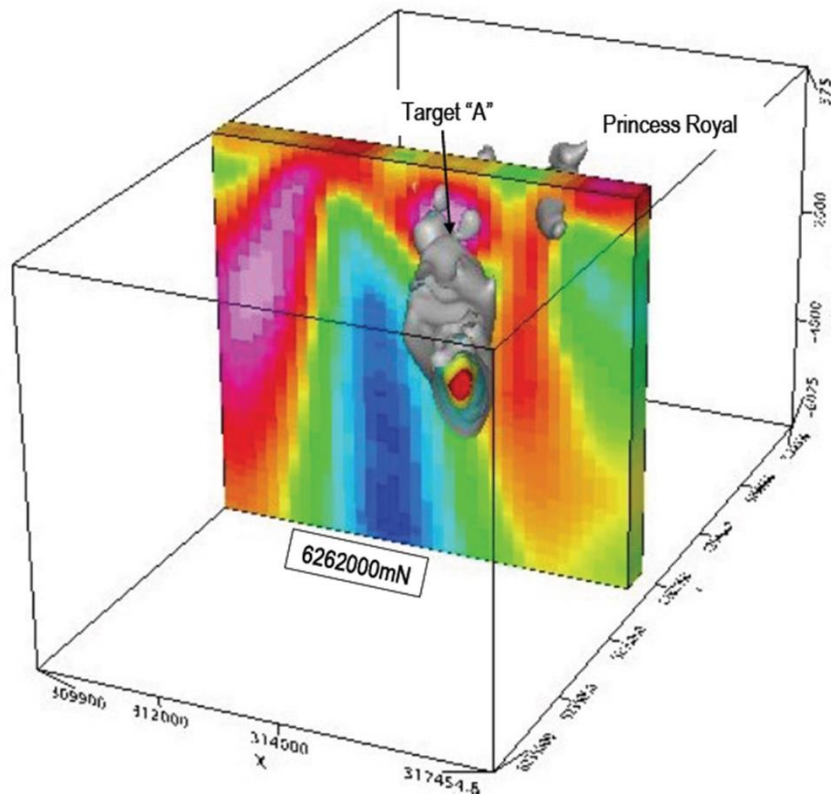


Figure 2: 3D Model viewed to the NW showing targets A in relation to Princess Royal. The large magnetic trends that coincide with a strongly conductive MT/AMT zone at Target A is similar to a smaller conductive zone below Princess Royal mineralisation.

The purpose of this report was to:

- Review and comment on the nature of each of the MT/AMT and the magnetic structures and comment on their coincidence.
- Comment on the potential relationship between Targets A & B and the smaller AMT and magnetic structure at the historic Princess Royal workings.
- Discuss whether these structures potentially image the source and plumbing systems for sulphide mineralisation at Princess Royal.
- Integrate these geophysical constraints into the model for the Princess Royal/Burra Cu-Ni-Co-REE-Au mineral system proposed in an earlier ASX announcement (October 4, 2018).

Data discussed in this report, support the interpretation that mineralisation at Burra is related to the mantle plume induced dispersal of the late Precambrian supercontinent called Rodinia between ~800 and 850 Ma ago.

The same plume metallogenic event was responsible for formation of the Jinchuan deposit in China (Mao et al., 2019), one of the three largest Cu-Ni-PGE (platinum group element) deposits in the world, containing more than 550 Mt with 1.1 wt.% Ni and 0.7 wt.% Cu.

Although the supergene copper resource has been exploited at Burra, the potential for deeper sulphide-hosted Cu-Ni-Co with associated Au and PGE has not been tested.

The shallow conductive MT/AMT magnetic structures recently reported by Ausmex Mining Group Limited are accessible by drilling and provide targets to test the presence of such ultramafic sourced mineralisation.

4. Princess Royal Deposit

The Princess Royal Deposit (Figure 3) in the Burra district of South Australia. Copper deposits in the district were discovered in 1843 and subsequently worked by the S.A. Mining Association, who obtained some 234,600 tons of ore of approximately 22 % grade. The mine finally closed in 1877 due to cessation of mining and a drop in the price of copper.

According to Brett (1956) the host rocks comprise a sequence of marbles, limestone, dolomites, fluvioglacials, quartzites and shales of Sturtian and Torrensian age. They are folded into a series of gently north-pitching folds. Folding is intense in the vicinity of the Burra Mine and the Princess Royal Mine, where a closed dome structure occurs. Strike faulting along the axes of anticlines is quite prominent.

The only igneous rock reported was a "feldspar porphyry", lying about ~1 km west of the Burra Mine. Copper mineralisation consists of mesothermal veins of chalcopyrite, bornite and pyrite in a gangue of calcite, quartz with occasional barite is common throughout the area. These veins commonly occur in reverse strike faults. According to Brett (1956) supergene carbonate derived from the primary mineralisation, that is common in the area, is believed to have formed by the precipitation of downward percolating acid copper solutions with carbonate wall-rock.

At the Princess Royal Mine, low grade veins occur in a brecciated and shattered zone at the axis of a dome structure, while at the Burra Mine, low grade veins occur in breccia between two strike faults.

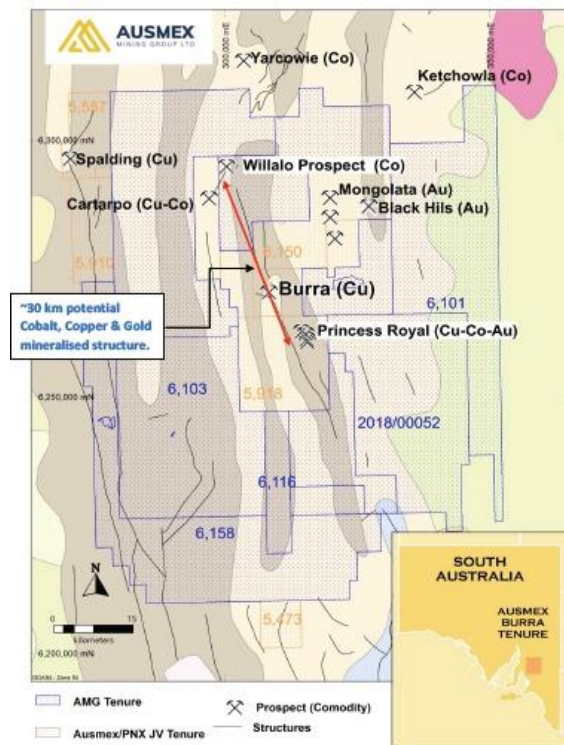
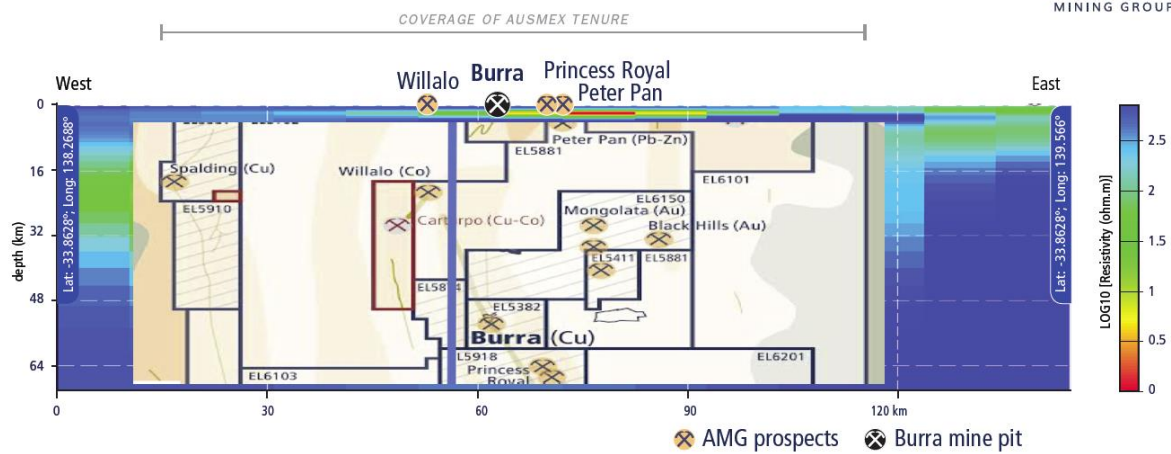


Figure 3: Map showing locations of Black Hill, Willalo and Princess Royal in Ausmex tenure in the Burra Area.

The recent AusLAMP (**A**ustralian **L**ithospheric **A**rchitecture **M**agnetotelluric **P**roject) survey conducted for Ausmex (ASX Market Releases 13 March, 2018; 5 July 2018) has identified a large conductive "MT flare" (~ 100 km in diameter) within the mid-to-lower crust directly beneath Ausmex's tenure at Burra. This MT anomaly is shown in Figure 4.

Cross-Section Looking North



Cross-Section Looking East

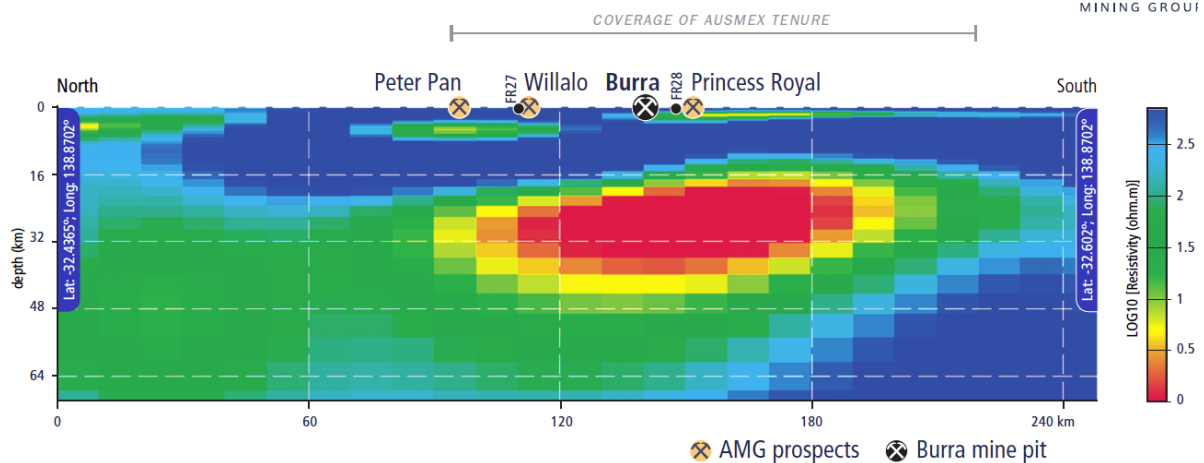


Figure 4: Large conductive MT flare (~ 100 km in diameter) within the mid-to-lower crust directly beneath Ausmex's tenure at Burra (cf., Heinson et al., 2018).

5. Imaging Conductive Structures

The conductive zones below the Burra mineralisation shown in Figures 1 and 2, and in Figures 5 to 7, provide a direct link with the conductive MT flare previously imaged in the mid-crust beneath Burra (Figure 4).

As target A correlates with known mineralisation at Princess Royal, it is likely that the zones of high electrical conductivity also reflect the presence of mineralisation at depth.

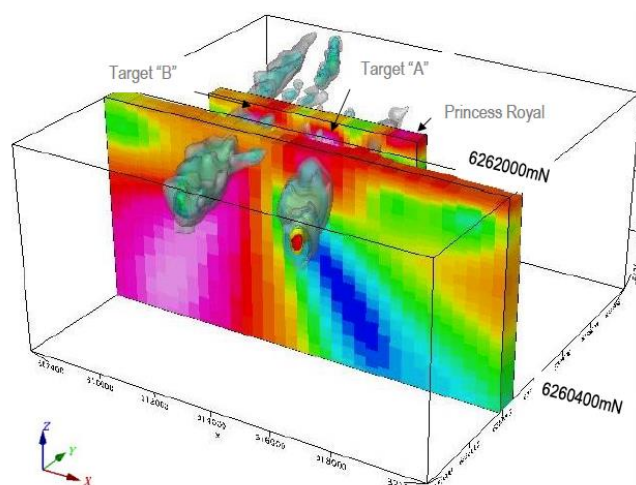


Figure 5: Model viewed to the NW showing targets A and B in relation to Princess Royal Deposit. Targets A and B are seen as large magnetic trends that coincide with a strongly conductive MT/AMT zone that extends to depth. Target A is several km in strike length and extends from near surface to ~1.7 km.

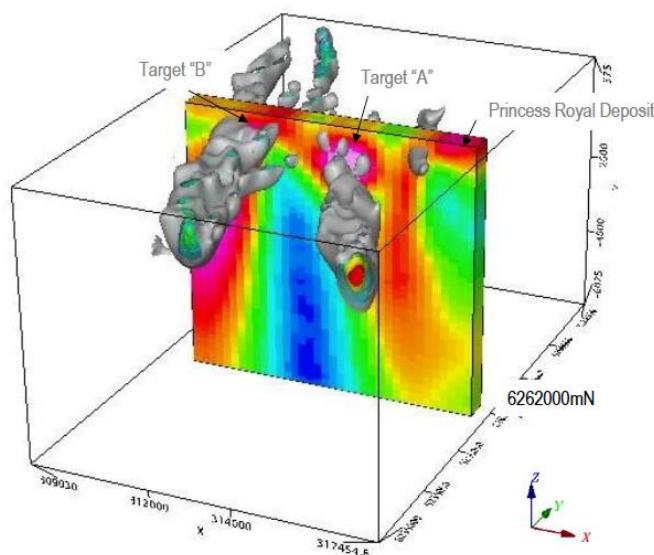


Figure 6: Model viewed to the NW showing targets A and B in relation to Princess Royal Deposit. Targets A and B are seen as large magnetic trends that coincide with a strongly conductive MT/AMT zone that extends to depth.

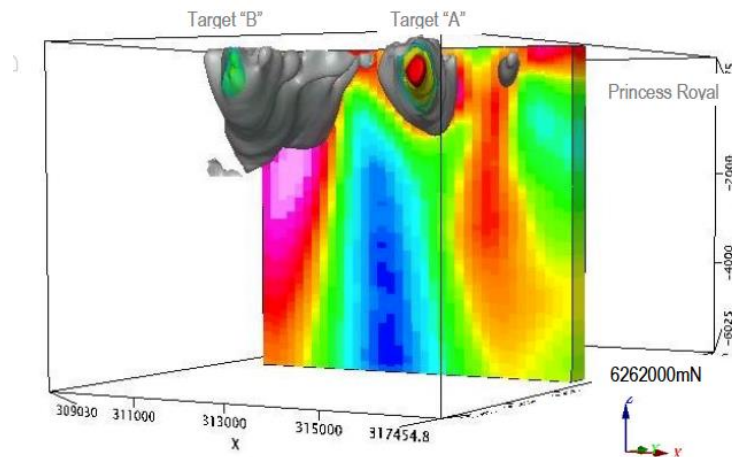


Figure 7: Model viewed to the NW showing targets A and B in relation to Princess Royal Deposit.

6. Geodynamic Controls on the Burra Mineral System

In an earlier ASX release (October 4, 2018) it was suggested that mineralisation at Burra and at the giant Jinchuan deposit, which is of similar age, was associated with the same magmatic plume event that caused the break-up of Rodinia.

A recent publication on the Jinchuan deposit by Mao et al., (2019) presents geochemical and minerals system data that support this hypothesis. Furthermore, Mao et al., (2019) suggested that the Jinchuan mineral system was fed by multiple magmatic conduits (Figure 8).

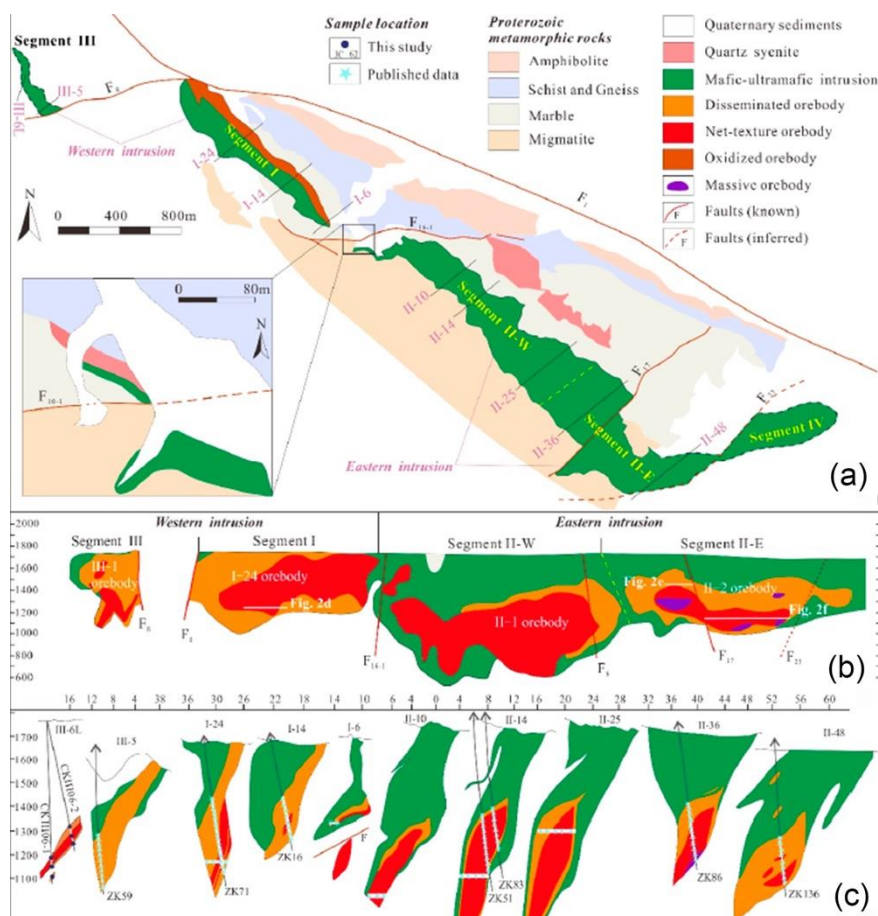


Figure 8: (a) Map of Jinchuan mineral system showing lenticular pipe-like feeders that are similar to the conductive structures mapped at Burra (from Mao et al., 2019).

In view of the geodynamic connection between Burra and Jinchuan (see below) the conductive pipes imaged below Burra could therefore be related to the magmatic plumbing system that provided conduits for metal migration into the Burra mineral system.

7. Geochemical Comparison of Burra and Jinchuan

Geochemical data use in this report are presented in Tables 1-5. The initial data were analysed by ICPOES following a four-acid digest. Gold was determined by 50 g fire assay with an AA finish.

At the request of Ausmex, the REEs for samples from Princess Royal were subsequently determined by Li borate fusion digestion and ICPMS analysis.

Ausmex Ltd. - The Burra Mineral System

Table 1: Selected element data for Princess Royal Rock Chips

	Au ppm	Ag ppm	Ba ppm	Cu ppm	Co ppm	Li ppm	Ni ppm	P ppm	Sc ppm	Sr ppm	V ppm	Y ppm	Zn ppm	Zr ppm	Pb ppm
BUPR0001	6.9	14	10900	31900	<10	<100	10	290	<10	280	20	10	110	10	<20
BUPR0002	0.055	2	2270	11700	<10	100	<10	130	<10	80	10	<10	20	<10	<20
BUPR0003	0.133	2	2020	19600	<10	<100	10	210	<10	50	10	<10	50	<10	<20
BUPR0004	0.113	2	3240	35300	<10	<100	20	300	<10	120	10	<10	70	<10	<20
BUPR0005	0.182	1	19800	61200	<10	<100	10	90	<10	450	<10	<10	190	<10	<20
BUPR0006	0.315	9	5660	>100000	<10	<100	10	110	<10	500	<10	<10	150	<10	<20
BUPR0007	0.26	1	12900	80000	10	<100	20	260	<10	270	20	<10	210	10	20
BUPR0008	0.03	<1	1620	67500	<10	<100	<10	90	<10	140	10	<10	30	<10	<20
BUPR0009	0.011	<1	9680	56300	<10	<100	<10	170	<10	410	10	<10	20	<10	<20
BUPR0010	0.012	<1	10300	3450	10	<100	20	2290	<10	320	80	10	1140	<10	<20
BUPR0011	0.126	2	7610	27900	10	<100	10	510	<10	1150	10	<10	70	<10	<20
BUPR0012	0.007	<1	3210	49500	<10	<100	10	640	<10	1050	10	<10	70	10	<20
BUPR0013	<0.005	<1	4910	890	10	<100	<10	190	<10	100	10	<10	40	<10	<20
BUPR0014	0.299	2	7760	27000	10	<100	10	120	<10	160	40	<10	50	<10	<20
BUPR0015	0.156	<1	2520	>100000	40	<100	30	240	<10	170	80	10	160	20	<20
BUPR0016	0.093	<1	3330	45100	30	<100	<10	790	<10	1300	40	10	<20	50	30
BUPR0017	0.093	<1	5540	54100	40	<100	20	180	10	200	90	10	110	10	<20
BUPR0018	<0.005	1	260	15900	<10	<100	<10	140	<10	100	10	<10	50	<10	<20
BUPR0019	0.135	<1	18900	17500	<10	<100	<10	230	<10	880	<10	<10	<20	<10	<20
BUPR0020	0.249	<1	15300	21500	<10	<100	<10	250	<10	530	10	<10	230	<10	<20
BUPR0021	0.215	<1	14400	42500	<10	<100	10	410	<10	1250	10	<10	100	<10	<20
BUPR0022	0.06	<1	300	11900	<10	<100	<10	200	<10	110	10	<10	30	<10	<20
BUPR0023	0.056	1	3830	85400	<10	<100	<10	290	<10	160	10	<10	60	<10	<20
BUPR0024	1.865	96	7040	89300	<10	<100	10	110	<10	1330	10	<10	460	<10	<20
BUPR0025	0.604	25	18100	43400	<10	<100	<10	130	<10	1070	<10	<10	230	<10	<20
BUPR0026	<0.005	1	2730	490	<10	<100	<10	610	<10	80	10	<10	20	<10	<20
BUPR0027	0.01	<1	43100	13300	2080	1200	360	520	<10	230	10	50	140	10	30
BUPR0028	<0.005	<1	33100	16100	2320	1500	440	380	<10	150	10	50	170	<10	30
BUPR0029	0.111	<1	6310	12800	110	<100	70	410	<10	450	40	30	190	10	<20
BUPR0030	0.061	<1	5150	12600	170	100	70	160	<10	210	10	10	80	<10	<20
BUPR0031	0.099	<1	1120	>100000	100	<100	50	290	<10	50	40	440	70	<10	<20
BUPR0032	0.241	<1	1300	>100000	220	<100	40	460	<10	190	40	780	100	10	<20
BUPR0033	0.178	<1	440	>100000	170	<100	50	420	30	80	150	160	390	20	<20
BUPR0034	0.114	<1	450	74800	80	<100	10	180	10	60	30	40	30	<10	<20
BUPR0035	0.373	<1	130	66300	60	<100	10	100	10	30	20	40	60	<10	<20
BUPR0036	0.441	<1	400	>100000	160	<100	20	220	10	130	30	110	120	<10	<20

BUPR0037	0.325	<1	2100	87800	130	<100	40	390	<10	340	50	330	100	20	40
BUPR0038	0.146	<1	6600	36200	160	<100	70	280	<10	680	60	60	140	10	<20
BUPR0039	1.005	37	7930	82900	10	<100	<10	<50	<10	570	10	10	1210	<10	<20
BUPR0040	0.042	<0.5	1570	17800	<1	10	3	20	<1	2870	1	<10	15	<5	6
BUPR0041	0.607	<0.5	3220	172500	132	10	42	610	5	502	70	460	137	24	11
BUPR0042	0.005	2.2	>10000	14600	2170	1240	393	490	5	173	14	40	104	<5	36
BUPR0043	<0.005	7.1	>10000	20300	3570	1950	435	510	5	126	11	40	119	<5	39
BUPR0044	0.026	1.8	>10000	12950	1535	720	242	320	3	195	12	50	96	<5	35
BUPR0045	<0.005	1.8	>10000	12500	2110	930	257	340	3	220	8	60	104	<5	42
BUPR0046	0.013	2.8	>10000	13500	2050	1040	291	390	5	226	11	80	114	<5	43
BUPR0047	0.005	1.7	>10000	14900	1955	1310	412	430	4	179	14	50	125	5	33
BUPR0048	0.023	0.7	>10000	15250	1560	1550	642	340	7	106	15	30	154	6	21
BUPR0049	<0.005	1.3	>10000	9470	1130	760	287	690	3	300	15	60	93	<5	22
BUPR0050	<0.005	2.9	>10000	18950	2490	1700	453	420	4	231	11	50	152	<5	47
BUPR0051	<0.005	2.5	>10000	19000	2890	1960	542	490	5	169	12	50	146	<5	39
BUPR0052	<0.005	3.5	>10000	18550	3100	1970	518	530	5	209	11	50	144	<5	46
BUPR0053	<0.005	<0.5	>10000	15800	1580	1490	577	310	4	128	13	30	148	<5	25
BUPR0054	<0.005	1.5	>10000	13350	1700	1100	312	330	3	176	9	50	125	<5	37
BUPR0055	0.029	<0.5	3560	3830	433	270	81	400	1	2200	21	10	118	<5	12
BUPR0056	0.41	<0.5	1800	11400	26	30	7	190	<1	1375	5	<10	37	<5	<2
BUPR0057	0.015	0.9	>10000	15450	1760	1400	480	350	4	174	13	30	143	5	26
BUPR0058	0.329	0.8	1270	45100	199	90	76	560	53	71	267	280	476	23	15
BUPR0059	0.012	8	150	35900	410	<100	290	560	10	660	20	140	720	60	30
BUPR0060	<0.005	1	120	26800	100	<100	60	1310	<10	1970	20	50	80	120	40
BUPR0061	<0.005	3	<50	44000	10	<100	20	510	<10	840	<10	10	30	10	20
BUPR0062	0.029	4	150	29000	510	<100	260	860	10	1320	20	110	460	40	20
BUPR0063	0.015	11	50	77400	50	<100	120	400	<10	380	10	70	370	40	30
BUPR0064	<0.005	<1	<50	1390	<10	<100	10	70	<10	30	60	<10	<20	<10	90
BUPR0065	<0.005	<1	70	610	40	<100	30	200	<10	30	40	<10	20	10	<20
BUPR0066	<0.005	1	<50	3370	20	<100	30	170	<10	80	30	20	20	10	<20
BUPR0067	0.006	<1	<50	100	<10	<100	<10	<50	<10	<10	40	<10	<20	10	<20
BUPR0068	<0.005	<1	<50	140	<10	<100	10	80	<10	10	50	<10	<20	10	<20
BUPR0069	<0.005	<1	50	450	10	<100	20	180	<10	10	20	10	<20	<10	<20
BUPR0070	<0.005	<1	<50	30	10	<100	10	120	<10	<10	10	<10	<20	10	<20
BUPR0071	0.067	2	80	80	290	<100	590	1730	10	30	30	20	<20	10	<20
BUPR0072	<0.005	<1	190	110	20	<100	180	1280	10	30	10	50	1280	30	230
BUPR0073	<0.005	<1	150	20	10	<100	30	1010	10	20	10	40	170	60	280

Ausmex Ltd. - The Burra Mineral System

BUPR00074	0.018	3	190	29200	20	<100	80	1100	10	30	30	10	80	40	<20
BUPR00075	0.08	28	50	>100000	10	<100	70	1180	10	40	90	10	120	10	<20
BUPR00076	0.02	4	110	30800	10	<100	60	1060	20	110	90	10	120	70	20
BUPR00077	0.019	2	90	32600	10	<100	60	1000	20	110	80	10	100	60	<20
BUPR00078	0.028	6	70	64100	20	<100	60	970	30	50	100	10	120	50	30
BUPR00079	0.005	<1	60	5870	80	<100	170	3990	10	230	30	50	180	430	<20
BUPR00080	0.075	22	120	53100	20	<100	60	1230	20	60	60	10	1130	30	<20
BUPR00081	0.052	8	410	30800	130	<100	380	850	20	80	70	20	750	50	20
BUPR00082	0.008	5	810	18800	30	<100	80	490	10	200	30	20	320	40	<20
BUPR00083	0.018	8	5520	12800	1340	700	230	310	<10	50	20	30	120	10	<20
BUPR00084	0.03	10	6880	11800	1350	800	250	260	<10	60	20	20	50	<10	20
BUPR00085	0.01	3	34000	12700	1530	900	330	340	<10	170	10	40	140	<10	40
BUPR00086	0.046	4	9190	20100	1480	2000	600	440	<10	250	40	20	150	<10	30
BUPR00087	0.388	8	8040	6420	2120	900	190	1060	10	250	40	30	110	10	20
BUPR00088	0.47	2	5200	5780	750	500	150	200	<10	130	20	10	60	<10	<20
BUPR00089	1.065	18	11600	29500	60	100	30	250	<10	490	10	<10	450	<10	<20
BUPR00090	0.624	2	7260	4830	810	500	220	320	<10	260	30	20	50	<10	<20
BUPR00091	1.225	6	7060	46200	20	<100	10	110	<10	2180	20	<10	950	<10	20
BUPR00092	2.62	23	8180	>100000	10	<100	10	220	<10	1920	20	<10	550	<10	20
BUPR00093	0.2	18	9390	17100	210	<100	460	3820	<10	1640	<10	<10	490	<10	<20
BUPR00094	0.535	11	12200	15600	190	<100	340	14300	<10	2860	10	<10	990	20	20
BUPR00095	0.023	1	3040	1310	20	<100	20	430	<10	60	30	10	20	20	<20
BUPR00096	0.016	2	14400	20200	30	<100	100	1520	10	290	40	20	110	70	<20
BUPR00097	0.01	3	6780	88900	10	<100	20	460	<10	110	<10	<10	30	<10	20
BUPR00098	<0.005	2	270	11100	20	<100	10	160	<10	<10	50	10	40	30	<20
BUPR00099	0.02	11	530	>100000	60	<100	90	2450	10	200	30	10	770	50	<20

Table 2: Selected element data for Peter Pan Rock Chips

	Au ppm	Ag ppm	Ba ppm	Cu ppm	Co ppm	Li ppm	Ni ppm	P ppm	Sc ppm	Sr ppm	V ppm	Y ppm	Zn ppm	Zr ppm	Pb ppm
BUPP0001	0.005	21.6	40	500	5	50	4	40		48	3		2280	6	11300
BUPP0002	0.005	0.5	10	18	4	20	3	130		59	2	10	2170	8	9340
BUPP0003	0.005	0.5	20	6	1		1	110	1.0	18	2	10	23		80
BUPP0004	0.005	0.5	30	325	10	10	28	230	2.0	61	14	20	4510	76	5160
BUPP0005	0.005	3.8	20	450	6	20	3	90		29	3	10	5540		11550
BUPP0006	0.005	2.6	120	252	7	20	12	260	3.0	71	14	30	1475	31	3540
BUPP0007	0.078	23.0	40	676	10	20	9	160	1.0	107	5	10	3800	41	29800
BUPP0008	0.005	16.4	10	1235	10	30	9	200		88	1	10	6970	29	18500
BUPP0009	0.024	18.1	30	353	7	20	8	90		54	3	10	3260	12	17450
BUPP0010	0.005	0.5	10	27	2		8	210		8	3		109		310
BUPP0011	0.020	0.5	30	8	3		6	120	1.0	9	5		43	26	248
BUPP0012	0.036	0.5	30	222	38	10	102	4370	1.0	26	45	20	405		6
BUPP0013	0.029	0.5	180	130	28		73	3210	3.0	21	32	20	259	22	11

Table 3: Selected element data for Black Hills Rock Chips

	Au ppm	Ag ppm	Ba ppm	Cu ppm	Co ppm	Li ppm	Ni ppm	P ppm	Sc ppm	Sr ppm	V ppm	Y ppm	Zn ppm	Zr ppm	Pb ppm
BUBH0001	0.02		130	102	425		599	1560	1.00	16.0	23.00	20.00	20.00		3.00
BUBH0002	0.02		110	50	130		166	170	3.00	120.0	19.00	30.00	18.00	19.00	
BUBH0003	0.01		110	13	64	10.00	36	160	1.00	43.0	13.00	10.00	38.00		2.00
BUBH0004	0.04		280	57	91		36	280	1.00	14.0	2.00	70.00	35.00		18.00
BUBH0005		2.50	10000	2160	1710		285	1830	5.00	1560.0	56.00	40.00	760.00	143.00	54.00
BUBH0006	0.01		9380	730	497	140.00	114	1290	6.00	417.0	24.00	30.00	257.00	34.00	22.00
BUBH0007	0.01		210	63	33	30.00	37	140	1.00	16.0	13.00	10.00	44.00	9.00	14.00
BUBH0008	0.32		110	327	108		158	1270	28.00	50.0	29.00	120.00	195.00	22.00	14.00
BUBH0009	0.01		20	16	4		8	80	2.00	7.0	15.00	10.00	13.00		

Table 4: Selected element data for Willalo Rock Chips

	Au ppm	Ag ppm	Ba ppm	Cu ppm	Co ppm	Li ppm	Ni ppm	P ppm	Sc ppm	Sr ppm	V ppm	Y ppm	Zn ppm	Zr ppm	Pb ppm
BUWI0001			40	16	10		15	110	2	12	6	10	26	<5	<2
BUWI0002			3460	358	1970		541	220	2	35	16	10	437	6	35
BUWI0003			10000	1315	6920	350	2570	870	2	232	113	230	1390	11	28
BUWI0004			8670	999	5660	1700	2090	750	1	206	83	250	1140	5	21
BUWI0005			4320	442	2790	1350	1010	400	1	114	42	110	542	<5	13
BUWI0006			10000	2120	4890	590	5130	740	1	531	108	110	2770	12	29
BUWI0007			5620	1470	5040	2220	2500	560	4	194	57	150	1285	13	26
BUWI0008			7740	429	1880	1510	644	550	2	190	46	80	455	7	16
BUWI0009			9490	1735	3710	280	5320	610	1	437	101	80	2670	9	28
BUWI0010			270	29	60	2090	42	80	1	25	16	<10	30	11	3
BUWI0011			320	47	81	20	109	130	5	66	75	10	65	84	11
BUWI0012			50	206	40	40	56	2160	9	17	79	30	37	66	8

Table 5: Rare Earth Element concentrations (ppm) for rock chip samples from Princess Royal

	La	Ce	Pr	Nd	Sm	Eu	Gd	Tb	Dy	Ho	Y	Er	Tm	Yb	Lu	Ce/Ce*	Y/Ho	Zr/Hf
BUPR0001	8.30	14.90	2.30	9.90	2.30	0.43	2.33	0.34	1.82	0.38	11.00	1.07	0.14	0.99	0.17	0.81	28.95	38.00
BUPR0002	0.60	1.10	0.17	0.70	0.17	0.03	0.21	0.04	0.20	0.05	1.70	0.13	0.02	0.13	0.02	0.82	34.00	
BUPR0003	0.70	1.20	0.19	0.80	0.19	0.04	0.24	0.04	0.24	0.06	2.40	0.16	0.03	0.14	0.03	0.78	40.00	
BUPR0004	0.70	1.00	0.16	0.80	0.22	0.05	0.39	0.06	0.37	0.11	4.30	0.35	0.04	0.29	0.05	0.70	39.09	30.00
BUPR0005	0.90	1.40	0.21	0.90	0.27	0.03	0.21	0.03	0.09	0.01	0.50	0.05		0.06	0.01	0.75	50.00	
BUPR0006	1.00	1.10	0.12	0.50	0.15	0.03	0.20	0.02	0.07	0.01	0.60	0.05		0.06	0.01	0.65	60.00	30.00
BUPR0007	0.90	1.30	0.16	0.60	0.17	0.03	0.14	0.02	0.10	0.03	0.80	0.08	0.01	0.08	0.01	0.77	26.67	37.50
BUPR0008	0.50	0.80	0.07	0.30	0.05	0.03	0.07	0.01	0.04		0.20					0.91		
BUPR0009	0.40	0.70	0.07	0.40	0.11	0.03	0.12	0.01	0.05	0.01	0.30					0.94	30.00	
BUPR0010	2.80	4.10	0.54	2.10	0.50	0.03	0.63	0.11	0.60	0.14	6.10	0.42	0.05	0.37	0.05	0.76	43.57	30.00
BUPR0011	10.30	15.00	1.82	7.30	1.90	0.03	1.18	0.11	0.08	0.01	1.20	0.06	0.03	0.25	0.10	0.78	120.00	
BUPR0012	1.40	2.40	0.30	1.30	0.44	0.07	0.45	0.06	0.23	0.04	1.30	0.11	0.01	0.08	0.01	0.86	32.50	30.00
BUPR0013	1.00	2.60	0.30	1.30	0.30	0.03	0.39	0.05	0.35	0.08	1.90	0.22	0.03	0.20	0.03	1.14	23.75	30.00
BUPR0014	3.40	6.00	0.80	3.30	0.72	0.10	0.75	0.12	0.62	0.13	3.40	0.36	0.05	0.33	0.05	0.85	26.15	35.00
BUPR0015	4.20	9.60	1.26	5.50	1.58	0.41	1.75	0.29	1.76	0.39	10.10	1.11	0.17	1.09	0.18	1.00	25.90	37.00
BUPR0016	21.20	40.80	4.69	17.40	4.06	1.28	3.82	0.55	2.72	0.51	14.10	1.35	0.18	1.26	0.19	0.95	27.65	33.85
BUPR0017	1.80	3.60	0.44	1.90	0.66	0.20	1.27	0.24	1.49	0.35	10.00	1.03	0.16	1.09	0.18	0.95	28.57	40.00
BUPR0018	0.60	1.10	0.17	0.60	0.14	0.04	0.16	0.02	0.11	0.02	0.70	0.06	0.01	0.05	<0.01	0.82	35.00	
BUPR0019	1.70	2.50	0.25	0.90	0.24	0.03	0.40	0.04	0.11	0.02	0.60	0.05	0.01	0.09	0.02	0.83	30.00	30.00
BUPR0020	2.70	4.20	0.40	1.20	0.18	0.03	0.25	0.03	0.11	0.02	0.60	0.05	0.01	0.05	0.01	0.87	30.00	
BUPR0021	11.40	15.90	1.38	3.70	0.59	0.03	0.60	0.07	0.20	0.03	1.10	0.09	0.02	0.12	0.03	0.82	36.67	23.33
BUPR0022	1.20	3.10	0.35	1.70	0.48	0.13	0.73	0.11	0.74	0.14	4.20	0.43	0.06	0.37	0.05	1.14	30.00	30.00
BUPR0023	0.50	1.10	0.14	0.60	0.22	0.03	0.27	0.04	0.18	0.03	1.10	0.11	0.02	0.14	0.02	0.99	36.67	30.00
BUPR0024	3.60	0.90	0.13	1.00	0.83	0.03	1.35	0.17	0.07	0.01	1.60	0.11	0.05	0.35	0.12	0.18	160.00	
BUPR0025	4.30	0.50	0.07	1.10	1.15	0.03	2.08	0.23	0.04	0.01	2.00	0.16	0.07	0.46	0.18	0.09	200.00	
BUPR0026	1.40	3.20	0.46	1.90	0.42	0.07	0.42	0.06	0.33	0.07	1.70	0.20	0.02	0.15	0.03	0.96	24.29	35.00
BUPR0027	33.80	1830.00	24.60	121.00	35.40	6.27	21.90	3.63	18.40	3.38	50.00	9.58	1.51	11.20	1.68	14.64	14.79	35.71
BUPR0028	27.60	1095.00	23.70	118.50	36.20	6.43	22.30	3.58	18.70	3.40	56.30	10.05	1.58	11.55	1.77	9.61	16.56	
BUPR0029	4.90	36.60	1.58	7.90	2.39	0.53	3.66	0.50	3.11	0.81	30.10	2.28	0.31	1.90	0.32	3.17	37.16	40.00
BUPR0030	2.50	46.10	1.20	6.30	2.05	0.39	2.38	0.33	1.95	0.43	11.90	1.19	0.17	1.13	0.17	6.41	27.67	35.00
BUPR0031	11.30	14.70	6.22	96.30	99.10	26.70	124.50	19.30	110.50	23.80	439.00	74.70	13.05	90.80	15.40	0.42	18.45	
BUPR0032	13.80	28.30	11.35	177.50	163.00	45.20	228.00	32.90	178.00	36.70	762.00	100.00	13.85	84.70	13.60	0.51	20.76	44.00
BUPR0033	8.70	46.40	7.34	55.50	21.20	5.74	32.10	5.13	31.00	6.67	151.00	19.05	2.75	17.65	2.71	1.31	22.64	38.00
BUPR0034	21.00	87.40	10.60	55.20	12.45	2.81	13.60	2.03	11.20	2.27	46.20	6.50	0.97	6.43	0.98	1.41	20.35	55.00
BUPR0035	6.80	23.70	4.07	25.50	8.58	2.22	11.60	1.91	10.95	2.36	46.80	6.63	0.99	6.30	0.95	1.07	19.83	35.00

Ausmex Ltd. - The Burra Mineral System

BUPR0036	11.10	16.40	6.12	38.10	13.80	3.94	24.00	4.00	23.40	5.07	115.50	13.45	1.91	11.60	1.74	0.47	22.78	40.00
BUPR0037	6.10	24.50	6.51	107.00	91.30	24.90	119.00	18.30	93.70	20.10	354.00	57.90	9.44	61.70	10.30	0.83	17.61	40.00
BUPR0038	4.00	10.30	1.95	21.20	14.65	4.13	23.40	3.39	16.40	3.22	65.80	7.58	0.98	4.74	0.73	0.89	20.43	37.50
BUPR0039	4.10	0.70	0.20	3.40	3.37	<0.03	3.64	0.50	2.13	0.47	10.40	1.28	0.26	2.01	0.48	0.12	22.13	
BUPR0040	2.30	1.50	0.16	1.00	1.41	<0.03	0.35	0.04	0.07	0.01	4.40	0.06	0.02	0.16	0.05	0.43	440.00	10.00
BUPR0041	13.60	18.00	5.67	63.90	48.80	14.05	90.30	12.45	74.20	15.20	512.00	40.80	5.16	29.80	4.54	0.50	33.68	40.00
BUPR0042	35.40	1205.00	27.00	139.50	43.40	7.34	25.60	3.99	21.50	3.66	52.00	10.65	1.74	12.50	1.81	8.93	14.21	30.00
BUPR0043	32.50	1215.00	23.40	123.00	37.50	6.46	23.30	3.48	18.55	3.23	51.10	9.58	1.51	10.55	1.52	10.18	15.82	30.00
BUPR0044	32.20	889.00	26.10	137.50	42.30	7.24	26.30	3.96	21.10	3.73	54.90	10.70	1.73	12.25	1.78	6.95	14.72	25.00
BUPR0045	45.10	1080.00	38.20	204.00	60.10	10.50	37.30	5.48	29.40	5.21	70.40	14.90	2.35	16.55	2.39	5.85	13.51	
BUPR0046	56.60	1040.00	41.90	220.00	63.60	11.35	41.80	6.16	33.30	6.02	90.90	17.25	2.71	18.65	2.76	4.92	15.10	35.00
BUPR0047	32.30	1770.00	23.10	119.00	36.20	6.46	22.70	3.66	19.10	3.33	49.40	9.91	1.60	11.40	1.64	14.99	14.83	40.00
BUPR0048	27.50	2050.00	12.80	64.00	19.75	3.58	13.15	2.24	11.65	2.12	38.00	6.22	1.00	7.23	1.04	26.34	17.92	50.00
BUPR0049	498.00	1070.00	113.50	410.00	63.50	10.75	38.10	4.83	24.30	4.10	64.30	11.25	1.67	11.55	1.65	1.05	15.68	40.00
BUPR0050	47.80	1775.00	30.10	155.00	45.60	7.95	28.20	4.38	22.80	3.95	62.70	11.60	1.88	12.90	1.83	11.01	15.87	
BUPR0051	28.40	2030.00	23.00	120.50	37.30	6.54	23.20	3.61	19.00	3.35	51.60	9.61	1.55	11.05	1.59	18.01	15.40	
BUPR0052	30.30	1485.00	27.80	145.50	45.20	8.03	27.10	4.19	22.40	3.84	53.90	11.05	1.79	12.80	1.82	11.34	14.04	
BUPR0053	22.60	1350.00	15.10	76.60	24.10	4.14	14.55	2.35	12.30	2.16	33.00	6.44	1.04	7.52	1.06	17.07	15.28	30.00
BUPR0054	37.10	918.00	29.40	158.00	46.10	8.13	29.80	4.47	23.70	4.19	58.20	12.05	1.91	13.30	1.96	6.33	13.89	
BUPR0055	7.40	181.00	3.07	15.40	5.33	<0.03	2.99	0.44	2.23	0.39	9.10	1.11	0.19	1.38	0.22	9.18	23.33	25.00
BUPR0056	1.20	11.00	0.25	1.40	0.92	<0.03	0.44	0.05	0.20	0.03	2.40	0.09	0.02	0.14	0.03	4.63	80.00	20.00
BUPR0059	10.30	21.70	2.96	13.30	4.35	1.58	17.75	4.52	33.00	6.90	155.00	20.50	3.21	22.50	3.63	0.94	22.46	41.15
BUPR0060	25.50	53.60	6.53	26.40	6.92	1.64	11.30	2.36	15.80	3.24	64.70	9.95	1.70	12.15	2.02	0.98	19.97	41.75
BUPR0061	5.60	12.60	1.69	7.40	1.78	0.36	1.95	0.33	2.18	0.48	10.60	1.67	0.29	2.35	0.40	0.98	22.08	40.00
BUPR0062	8.20	18.70	2.60	11.70	3.61	1.28	12.75	3.24	23.30	4.89	119.00	15.00	2.38	16.85	2.76	0.97	24.34	47.50
BUPR0063	6.70	13.90	1.83	7.70	2.35	0.80	8.32	2.19	16.05	3.33	77.70	10.40	1.67	11.80	1.96	0.95	23.33	44.55
BUPR0064	0.80	1.70	0.22	1.00	0.30	0.26	0.38	0.07	0.38	0.08	1.90	0.21	0.03	0.21	0.04	0.97	23.75	
BUPR0065	1.40	3.20	0.50	2.10	0.71	1.17	0.91	0.15	0.92	0.16	3.90	0.44	0.07	0.42	0.07	0.92	24.38	
BUPR0066	5.20	14.20	2.25	10.00	3.48	5.62	4.06	0.67	3.88	0.72	16.80	1.92	0.27	1.77	0.25	1.00	23.33	
BUPR0067	0.40	0.80	0.11	0.40	0.12	0.14	0.18	0.03	0.15	0.03	0.70	0.07	0.01	0.08	0.01	0.91	23.33	
BUPR0068	1.20	2.70	0.39	1.60	0.44	0.65	0.63	0.12	0.64	0.13	3.20	0.32	0.05	0.26	0.03	0.95	24.62	
BUPR0069	2.00	4.80	0.74	3.30	1.26	1.81	1.43	0.24	1.41	0.26	5.70	0.68	0.10	0.60	0.08	0.95	21.92	
BUPR0070	1.80	3.70	0.51	2.00	0.52	0.90	0.57	0.09	0.51	0.09	2.30	0.27	0.03	0.23	0.04	0.92	25.56	35.00
BUPR0071	1.70	3.20	0.47	2.50	1.52	0.72	3.60	0.62	3.71	0.78	17.50	2.19	0.33	2.10	0.34	0.85	22.44	
BUPR0072	6.00	18.40	2.79	13.00	5.53	2.60	13.80	2.79	16.80	3.14	52.90	8.50	1.20	7.48	1.10	1.08	16.85	63.33
BUPR0073	3.80	14.00	2.16	10.70	5.07	2.33	13.10	2.66	15.90	2.92	43.60	7.92	1.14	7.23	1.06	1.16	14.93	65.56
BUPR0074	0.90	2.50	0.41	2.20	0.71	0.22	1.28	0.21	1.18	0.23	6.00	0.59	0.08	0.53	0.09	0.99	26.09	126.67

Ausmex Ltd. - The Burra Mineral System

BUPR00075	5.10	10.40	1.38	6.00	2.09	0.59	2.87	0.49	2.60	0.45	10.20	1.31	0.18	1.23	0.18	0.93	22.67	47.50
BUPR00076	22.40	46.50	5.77	22.20	4.33	0.92	3.97	0.64	3.68	0.71	17.40	2.04	0.29	1.97	0.30	0.97	24.51	41.82
BUPR00077	24.30	49.80	6.20	23.70	4.26	0.83	3.32	0.50	3.02	0.57	14.00	1.66	0.24	1.64	0.26	0.96	24.56	43.68
BUPR00078	9.70	20.00	2.55	10.30	2.75	0.70	3.32	0.57	3.37	0.65	15.50	1.84	0.28	1.91	0.29	0.95	23.85	53.64
BUPR00079	17.70	35.40	4.90	20.90	5.95	1.59	10.80	1.67	9.75	2.01	60.80	5.77	0.79	4.88	0.80	0.91	30.25	78.52
BUPR00080	2.70	6.00	0.83	3.80	1.10	0.31	1.41	0.23	1.32	0.25	7.10	0.76	0.11	0.79	0.12	0.96	28.40	120.00
BUPR00081	10.40	21.50	2.70	10.90	2.95	0.96	5.47	0.84	5.32	1.12	29.90	3.11	0.44	2.77	0.41	0.96	26.70	45.88
BUPR00082	2.90	6.20	0.87	4.30	2.16	0.84	5.13	0.79	4.55	0.90	22.00	2.51	0.34	2.15	0.32	0.94	24.44	70.00
BUPR00083	2.70	76.00	2.83	23.00	11.60	2.58	11.55	1.76	9.72	1.79	32.10	5.31	0.85	5.97	0.88	5.92	17.93	40.00
BUPR00084	2.90	73.90	3.03	25.10	13.10	2.93	12.45	1.89	10.50	1.85	29.00	5.39	0.85	6.17	0.91	5.37	15.68	
BUPR00085	28.70	894.00	24.30	128.00	38.80	6.70	23.90	3.66	19.50	3.46	47.40	10.05	1.68	11.85	1.72	7.62	13.70	30.00
BUPR00087	13.40	245.00	7.92	44.60	14.80	2.85	11.15	1.76	9.82	1.80	28.10	5.29	0.82	6.16	0.88	5.63	15.61	40.00
BUPR00088	8.60	216.00	4.07	19.90	5.94	1.09	4.37	0.69	3.74	0.69	9.10	2.08	0.34	2.43	0.37	8.79	13.19	
BUPR00089	0.80	14.70	0.34	1.90	0.70	<0.03	0.55	0.09	0.46	0.08	1.90	0.22	0.03	0.26	0.04	6.81	23.75	
BUPR00090	27.00	691.00	26.00	120.00	28.90	4.42	11.55	1.59	7.44	1.24	16.90	3.48	0.57	4.39	0.60	5.72	13.63	35.00
BUPR00091	3.20	5.50	0.24	1.70	2.45	<0.03	0.75	0.10	0.27	0.06	9.20	0.24	0.07	0.41	0.12	1.12	153.33	10.00
BUPR00093	3.80	26.20	1.05	5.60	3.08	<0.03	0.97	0.13	0.44	0.08	8.40	0.30	0.06	0.42	0.10	3.13	105.00	13.33
BUPR00094	3.00	4.80	0.46	2.50	1.73	<0.03	0.66	0.08	0.31	0.08	7.10	0.26	0.05	0.34	0.09	0.89	88.75	62.00
BUPR00095	7.30	13.90	1.76	7.00	1.53	0.72	1.84	0.32	1.91	0.34	8.60	0.81	0.10	0.51	0.06	0.91	25.29	
BUPR00096	12.10	27.30	3.00	12.00	3.07	0.66	4.68	0.74	4.08	0.79	22.50	2.05	0.28	1.56	0.25	1.07	28.48	48.10
BUPR00097	0.70	2.30	0.19	0.80	0.21	<0.03	0.14	0.02	0.09	0.02	0.70	0.06	0.01	0.07	0.01	1.50	35.00	
BUPR00098	2.00	2.70	0.49	2.20	0.58	0.24	0.85	0.16	1.02	0.22	6.20	0.65	0.10	0.65	0.10	0.64	28.18	103.33
BUPR00099	8.30	14.80	1.94	7.50	1.49	0.30	1.43	0.18	0.99	0.19	5.60	0.58	0.08	0.54	0.09	0.86	29.47	68.75

7.1 Trace Element Abundances

7.1.1 Nickel and Cobalt

Selected trace element abundances in rock chips from Princess Royal, Peter Pan, Black Hills and Willalo (Tables 1- 4) show the strong impact of a mafic to ultramafic source. This is illustrated in Fig. 9, which shows that Ni and Co are well correlated, ranging up to ~7000 ppm Ni and ~ 7000 ppm Co in samples from Willalo. The samples from Peter Pan are the least enriched in Ni and Co. Significantly elevated Ni and Co concentrations occur in samples from Willalo and Black Hills. Samples from Peter Pan are less anomalous, but nevertheless fall on the same covariation trend, which suggests a genetic relationship.

High concentrations of Ni and Co in the Willalo samples, are interpreted to indicate that Willalo is possibly located proximal to a mafic to ultramafic intrusion. In view of this, consideration should be given to undertake further soil and chip sample geochemistry, as well as evaluate magnetic and gravity data to document the existence of potential drill targets for Co mineralisation.

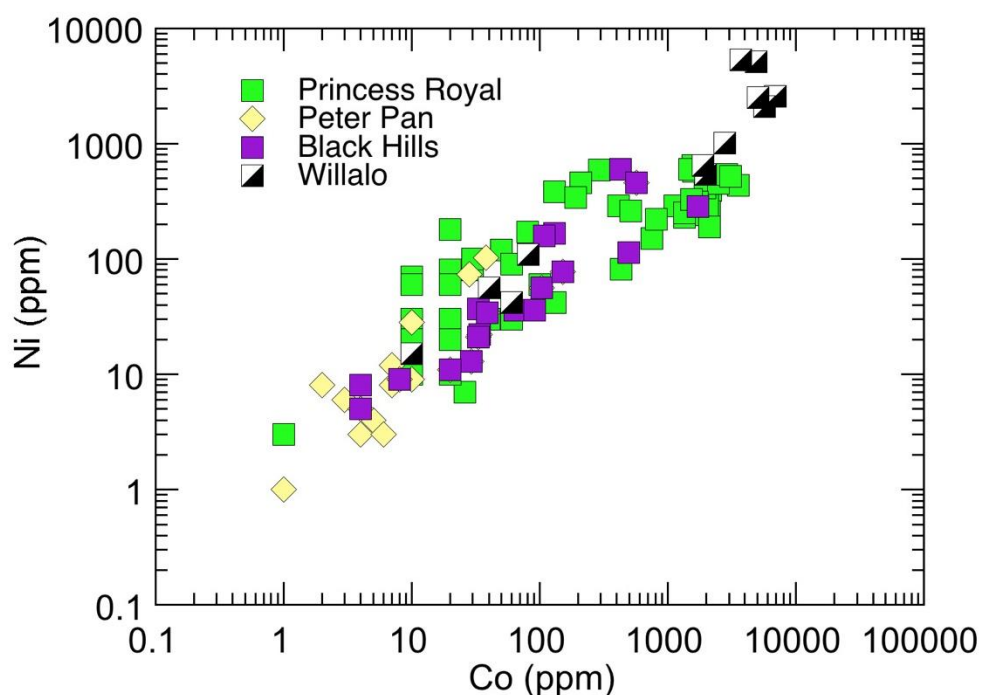


Figure 9: Co variation between Ni in chip samples from Ausmex's tenure in the Burra district. Significantly elevated Ni and Co concentrations occur in samples from Willalo, Black Hills and Princess Royal. Samples from Peter Pan are less anomalous but nevertheless fall on the same covariation trend which suggests a genetic relationship.

7.1.2 Copper and Cobalt

Covariation between Cu and Co in chip samples is shown in Figure 10. Data from Princess Royal, Willalo and Black Hills fall on the same fractionation trend, which suggests a genetic

relationship. However, deviations in Cu concentrations in samples from Princess Royal (with up to 100,000 to 200,000 ppm Cu, with between 1000 and 10,000 ppm Co) reflects a significant secondary enrichment in Cu. Samples from Peter Pan are less anomalous in Co and show elevated Cu values (up to 1000 ppm) at low Co concentrations (~10 ppm).

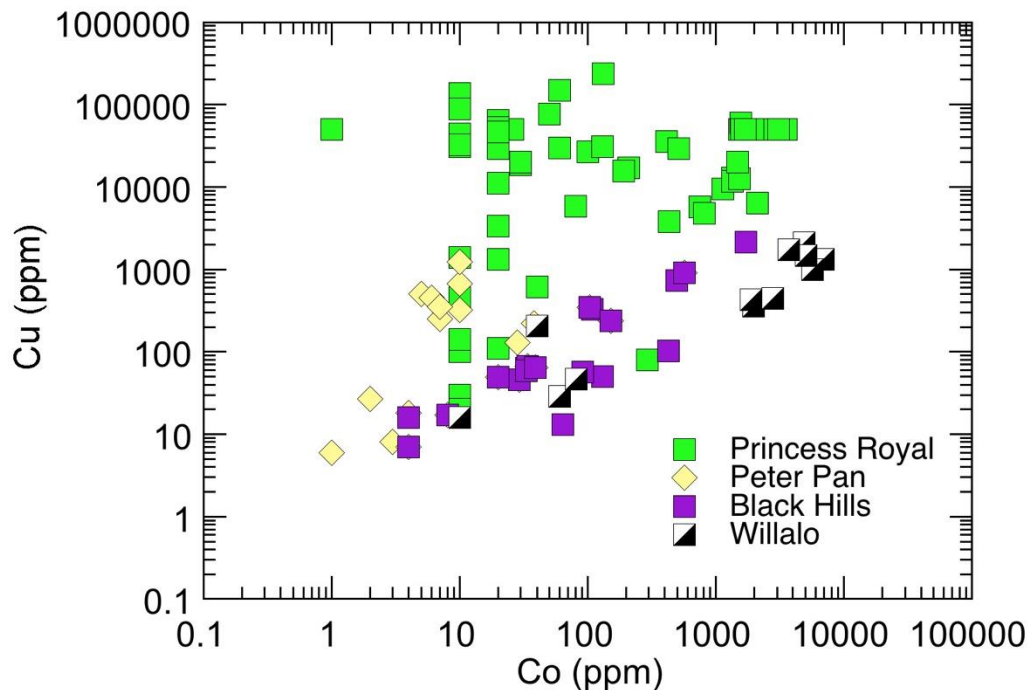


Figure 10: Covariation between Cu and Co in chip samples from Ausmex's tenure in the Burra district. Data from Princess Royal, Willalo and Black Hills fall on the same fractionation trend, which suggests a genetic relationship. However, deviations in Cu concentrations in samples from Princess Royal (with up to 100,000 to 200,000 ppm Cu, with between 1000 and 10,000 ppm Co) reflects a significant secondary enrichment in Cu. Samples from Peter Pan are less anomalous in Co and show elevated Cu values (up to 1000 ppm) at low Co concentrations (~10 ppm).

7.1.2 Zinc and Copper

Covariation between Cu and Zn in chip samples from AusMex's tenure in the Burra district are shown in Figure 11. Covariation between Cu and Zn in chip samples from Willalo, Peter Pan and Black Hills lie on the same fractionation trend. This suggests that systems are genetically related. However, deviations in Cu concentrations in samples from Princess Royal (with up to 100,000 to 200,000 ppm Cu, with low to high Zn (10 to 1000 ppm Zn), likely reflects significant secondary Cu enrichment. Peter Pan area is considered to be a potential target for hydrothermal Co and Zn mineralisation.

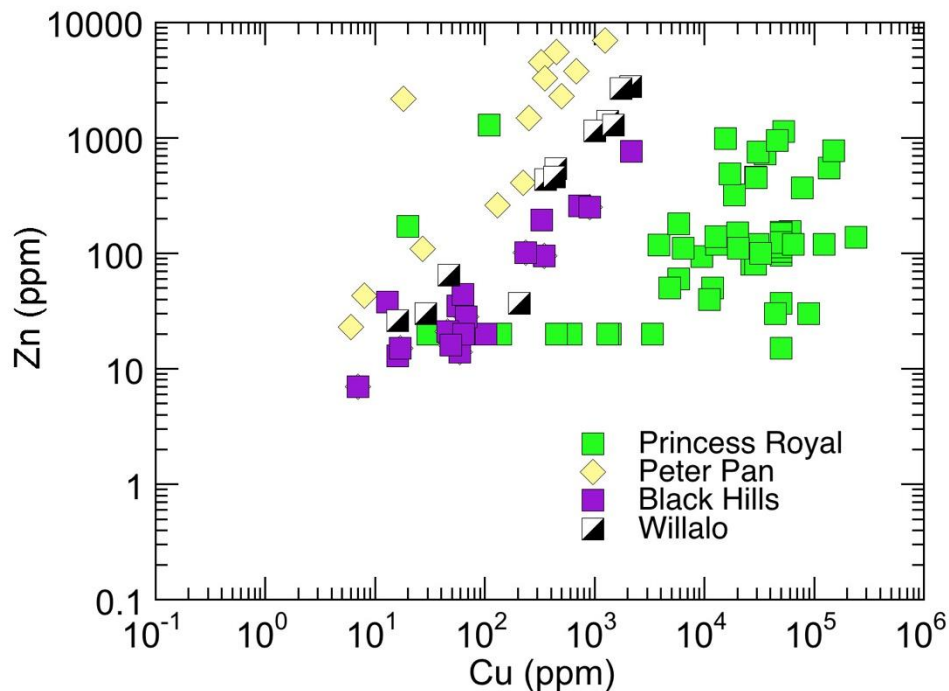


Figure 11: Covariation between Cu and Zn in chip samples from Ausmex's tenure in the Burra district. Data from Willalo, Peter Pan and Black Hills lie on the same fractionation trend, which suggests that systems are genetically related. However, deviations in Cu concentrations in samples from Princess Royal (with up to 100,000 to 200,000 ppm Cu, with low to high Zn (10 to 1000 ppm Zn) again, reflects a significant secondary enrichment in Cu.

7.2 CHARAC Ratio Systematics

Ratios of the high field strength elements Zr and Hf, as well as Y and the heavy rare earth element Holmium (Ho), are useful to evaluate the nature of hydrothermal processes in mineral systems. These so called CHARAC ratios (Y/Ho and Zr/Hf) enable magmatic source characteristics in mineral deposits to be distinguished from systems affected by hydrothermal processes (Bau, 1996).

If a geochemical system is characterized by CHARGE and-RADIUS-CONTROLLED (CHARAC) trace element behaviour, elements with similar charge and ionic radius, such as the twin pairs Y-Ho and Zr-Hf, should display coherent behaviour during crystallization and retain their respective chondritic ratios. Mantle-derived igneous rocks, for example, have Y/Ho and Zr/Hf ratios close to the ratios recorded by chondritic meteorites, viz. 28 and 38.

Carbonatites and alkaline igneous systems display this characteristic (de Andrade et al., 2002). These ratios are within error of values exhibited by mantle plume generated ocean island basalts (OIBs) viz., $Y/Ho = 27.7 \pm 2.7$ and $Zr/Hf = 36.6 \pm 2.9$ (Bau, 1996). Thus, they are useful indicators of mantle plume magmatism.

However, Y can be fractionated from Ho in medium-temperature F-rich aqueous fluids in hydrothermal systems due to fluoride complexation (Bau and Dulski, 1995; Buhn, 2008). Similar fractionation also occurs in F-rich peralkaline granitic melts (Bau and Dulski, 1995; Buhn, 2008).

7.2.1 Burra Y/Ho and Zr/Hf Systematics

Figure 12 shows covariation between Y/Ho and Zr/Hf ratios in samples from Princess Royal. The data range between super-chondritic and sub-chondritic values indicating that the mineral system has been affected by hydrothermal fluids containing fluorine, as F is the main ligand that can lead to Y fractionating from Ho.

Figure 13 shows covariation between Y/Ho and Y in samples from Princess Royal. Both low REE and high REE populations from Princess Royal define a broad trend of covariation due to fractionation of the REEs and Y by F-rich fluids.

Comparative Y/Ho and Zr/Hf data for the Jinchuan mineral system are shown in Figure 14.

F-induced hydrothermal effects to produce non-chondritic Y/Ho ratios are also seen in the Jinchuan population

Thus, the Y/Ho data clearly confirm the important role of fluorine complexation in the Princess Royal mineral system. This supports the interpretation that metals in the Jinchuan and Burra mineral systems were likely transported as F-complexes.

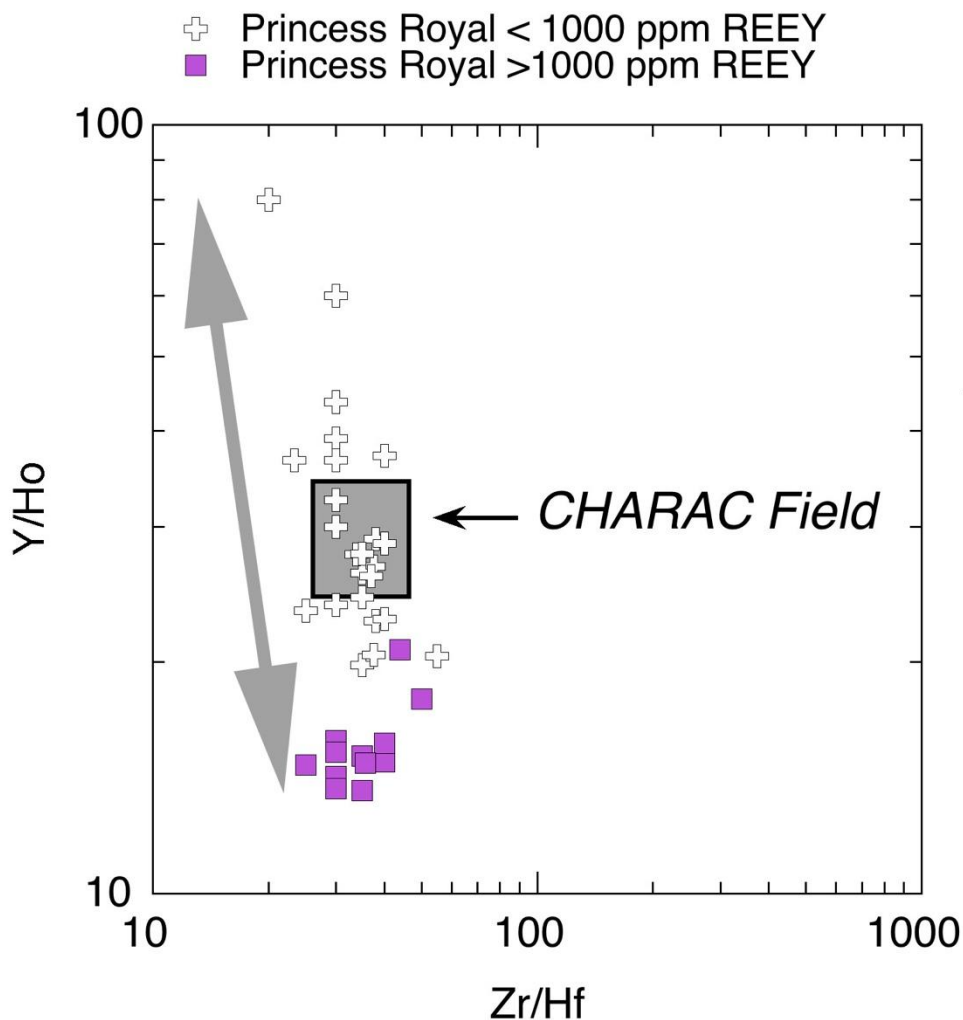


Figure 12: Covariation between Y/Ho and Zr/Hf ratios in samples from Princess Royal. The samples from Princess Royal show significant non-CHARAC behaviour. This is interpreted to indicate that the Princess Royal mineral system has been significantly affected by hydrothermal fluids containing fluorine, as F is the main ligand that can lead to Y fractionating from Ho. Fractionation path is shown by the grey double ended arrow.

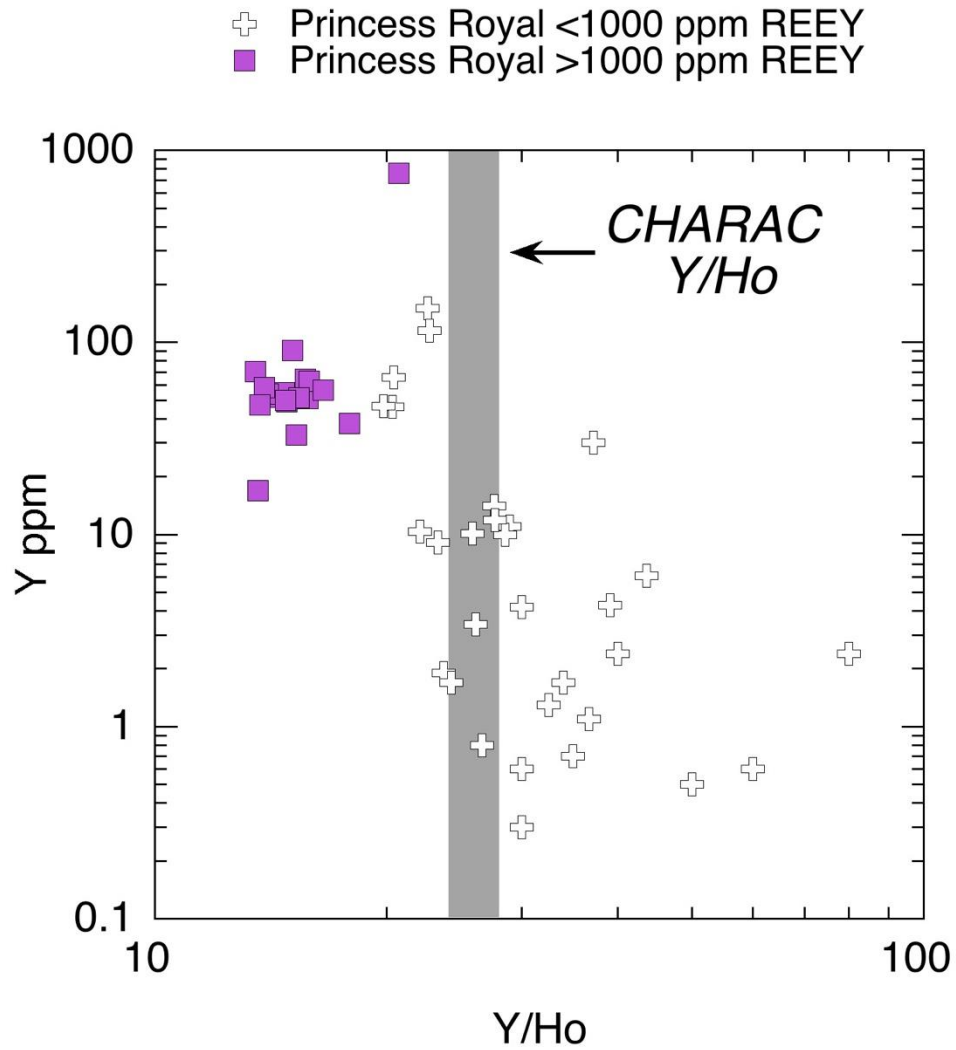


Figure 13: Covariation between Y/Ho and Y in samples from Princess Royal. Data define a broad trend of co-variation caused by fluid phase F induced fractionation of the REEs and Y.

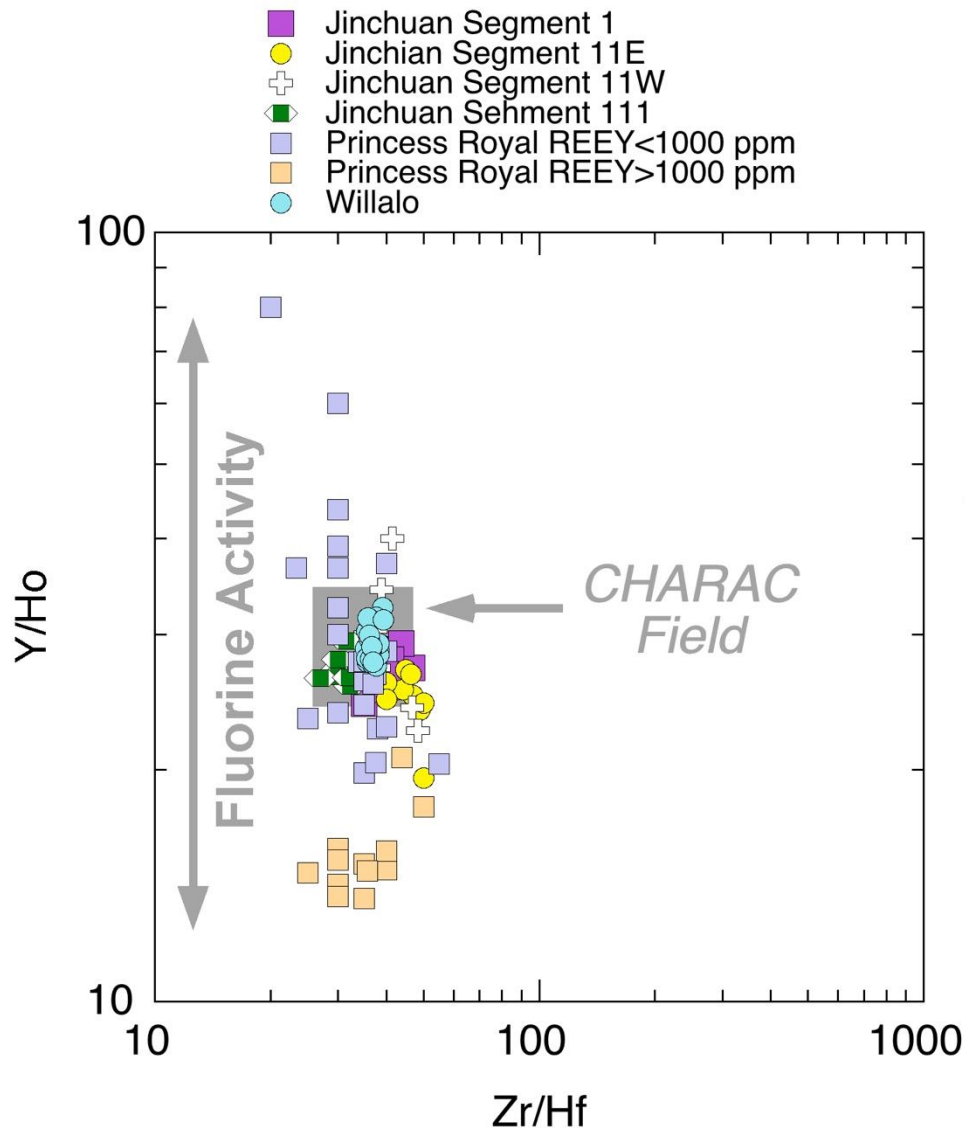


Figure 14: CHARAC Ratio plot comparing data from Jinchuan with Burra

7.3 La/Yb versus Total Rare Earth Projection

The La/Yb ratio (a proxy for LREE/HREE ratio) versus total REE diagram, devised by Loubert et al., (1972), is an extremely valuable projection to show REE sources.

Data for Princess Royal are shown in Figure 15. The Princess Royal REEs which were fractionated by halogen-rich fluids, plot in two distinct fields. The group with total REEs >1000 ppm falls within carbo-fluorothermal field. The low REE group extends from this field into that of fractionated alkaline intrusions. One sample (BUPR0049), plots in the carbonatite field.

This is interpreted to indicate that the fluids which transported the lanthanides and the transition metals (Co, Cu and Ni) into the Princess Royal mineral system were most likely derived from an alkaline igneous source that even contained carbonatites.

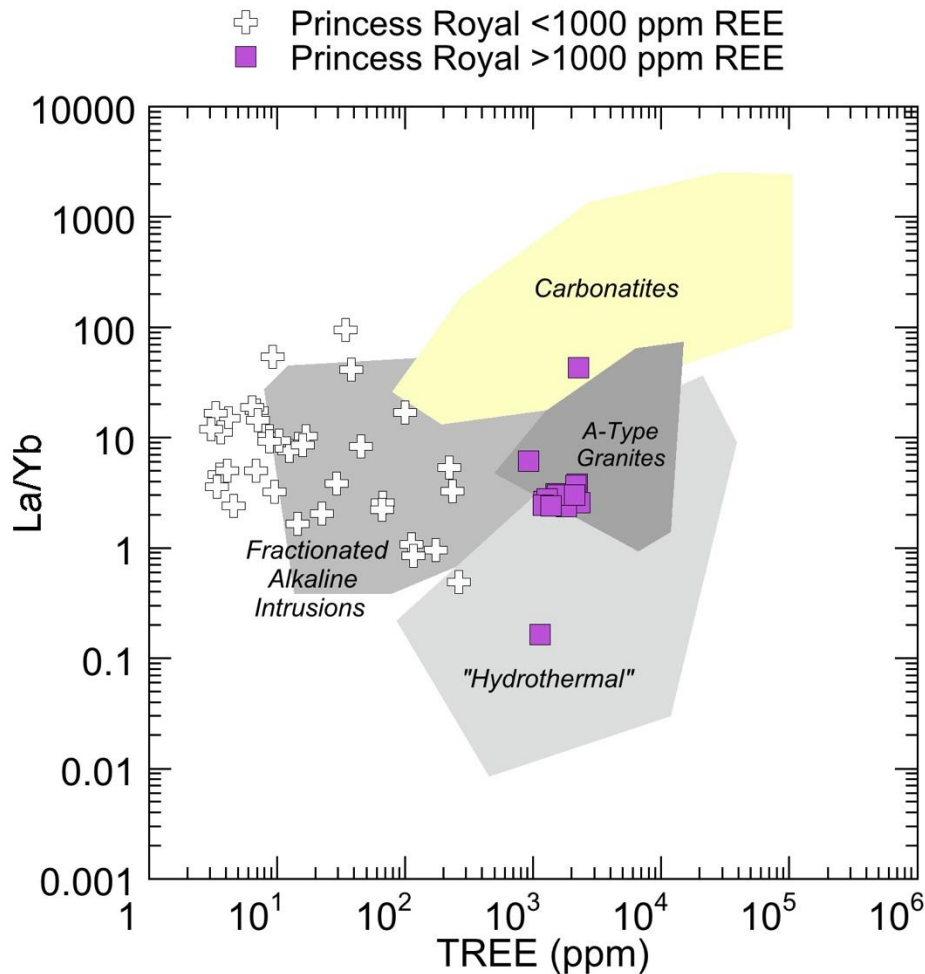


Figure 15: Variation in REEs shown by samples from Princess Royal. The group with total REEs >1000 ppm falls within carbo-fluorothermal field. The low REE group extends from this field into that of fractionated alkaline intrusions. One sample (BUPR0049), plots in the carbonatite field.

7.4 Fluid transport of Co and REEs

The presence of sub-chondritic Y/Ho ratios, Ce/Ce* anomalies and elevated Li concentrations indicates the involvement of halogen-rich hydrothermal fluids in the evolution of Princess Royal mineral system, with metals being derived from a mafic - ultramafic alkaline source.

Such halogen-rich fluid compositions are conducive to fluid - metal transport (Liu et al., 2011; Landis and Hofstra, 2012; Brugger et al., 2016) where metals are transported as aqueous complexes. Dissociation of these complexes in response to changes of the hydrothermal environment caused by a variety of processes, e.g., fluid-rock interaction, fluid mixing, cooling, or phase separation, results in the precipitation of minerals (Seward and Barnes, 1997).

The most stable oxidation state of cobalt in hydrothermal systems is Co(II), and thus Co(II) chloride complexes are inferred to be responsible for cobalt transport and deposition in ore-forming hydrothermal systems (Liu et al., 2011; Brugger et al., 2016). This is clearly the case in Idaho and most likely also at Princess Royal.

8. Role of Plume Magmatism in Generation of Mineral Deposits

8.1 Olympic Dam

The geodynamic framework for ~1590 Ma magmatism (Johnson and Cross, 1995) that generated the Olympic Dam deposit is interpreted to have involved an upwelling Mesoproterozoic mantle plume beneath the Gawler Craton (Betts et al., 2007). This deep-sourced upwelling plume provided heat for crustal melting to form the Gairdner Large Igneous Province (LIP) containing the Gawler Range Volcanics and the Hiltaba Granites. In addition, the plume also delivered metals and a volatile flux enriched in fluorine (Marks et al., 2014). This fluid composition played a major role in metal transport (McPhie et al., 2011). These fluorine-rich hydrothermal fluids are interpreted to have been responsible for the high metal content (including REEs) of the Olympic Dam deposit and they were crucial in enabling development of its polymetallic character. As a result, the mineralisation is enriched in fluorine and there is an intimate association between Cu sulphides and fluorite in the hematite-rich breccias (Roberts and Hudson, 1983; Oreskes and Einaudi, 1990; Haynes et al., 1995).

Magmatism associated with the event responsible for formation of the Olympic Dam mineralization at 1.59 Ga (1590 Ma) subsequently produced mineralisation in the Mary Kathleen Belt/Eastern successions in northern Australia at ~1.55 - 1.5 Ga and then in Idaho Co Belt at 1.46 Ga. In fact, reconstructions of Laurentia and Precambrian Australia at ~1.6 Ga place the Idaho Copper Belt immediately adjacent of the Mount Isa Block. Figure 16 shows that between 1.5 Ga and 1.3 Ga a plume track developed along the eastern margin of Precambrian Australia that enabled it to separate from western Laurentia (Betts et al. 2007, 2009).

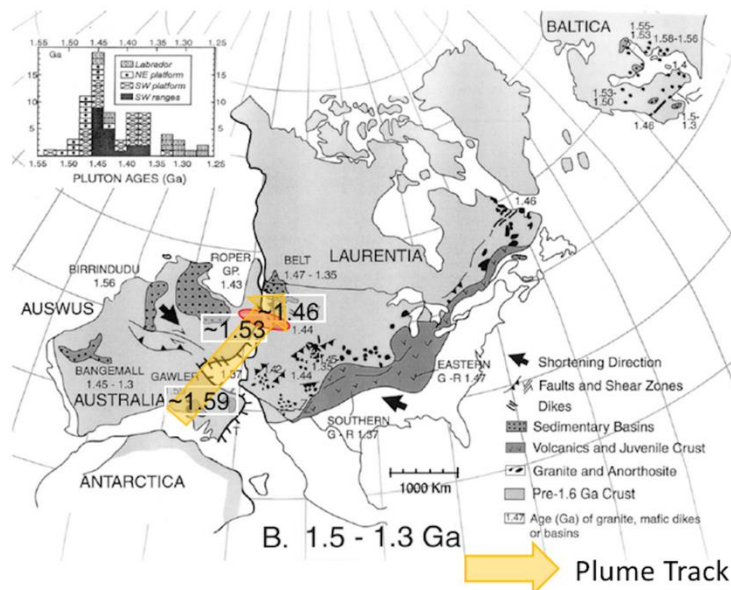


Figure 16: Reconstruction of Australia and Laurentia at 1.5 to 1.3 Ga. The pale orange arrow shows the trace of a plume track (Betts et al., 2007; 2009). The pink oval shows the approximate position of the Idaho Cobalt Belt in Laurentia and the location of Co systems in the Mount Isa Block. Timing of alkaline magmatism in the Mt Isa Block (U-Pb titanite) and in Idaho (U-Pb xenotime; Aleinikoff et al., 2014).

8.2 Burra Mineral System

Mafic plume related alkaline magmatism also occurred during the subsequent dispersal a younger supercontinent called Rodinia at ~820-830 Ma. This plume magmatism was responsible for generation of the ~820 Ma Gairdner Dyke swarm in South Australia (Sheraton and Sun, 1997; Huang et al., 2015, 2017).

However, Neoproterozoic Burra mineralisation formed at ~790 Ma: (Preiss et al., (2009), 800 Ma younger than Olympic Dam mineralisation (1590 Ma). Burra is located on the eastern margin of the Adelaide Rift, of the Gawler Craton and Curnamona Cratons. If these cratons were contiguous prior to rifting, then it is possible that the regional conductive anomaly in the deep lithosphere below Olympic Dam may have extended to the east and was rifted during formation of the Adelaide Rift.

However, the lithosphere lying east of the Gawler Craton also lies within the zone of impact of the postulated ~830 Ma mantle plume responsible for break-up of Rodinia (Figures 17 & 18). Magmatism associated with this plume event was responsible for generation of the Gairdner Large Igneous Province between ~820 Ma - 830 Ma in South Australia (Wingate, et al., 1998; Wang et al., 2010; Huang et al., 2015).

The conductive "MT flare" modelled below Burra is interpreted to represent a Neoproterozoic example of the plume generated metal-rich domain that formed below Olympic Dam during the Mesoproterozoic. This plume event could also have played a role in genesis of Olympic Dam mineral system, as Gairdner dykes also intrude this deposit (Huang et al., 2015).

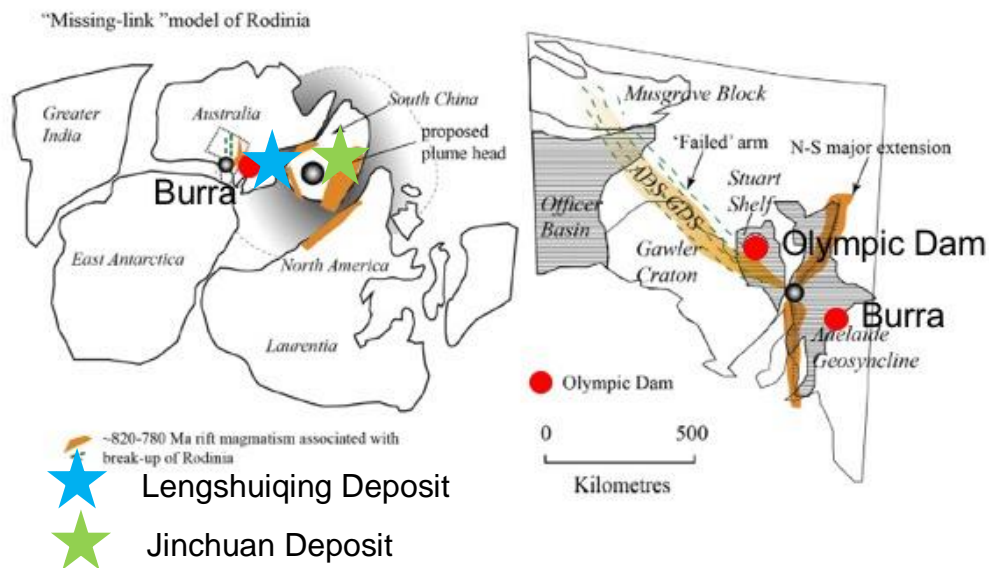


Figure 17: Modelled plume head responsible for breakup of Rodinia (after Huang et al., 2015). This model, based on geochronology and palaeomagnetic data, places the plume head below a microcontinent that broke away from Australia and Laurentia and eventually accreted with China. In Australia, the impact of alkaline and tholeiitic magmatism associated with this magmatic event extends as far as Broken Hill to the east (Wingate et al., 1998).

Tholeiitic and alkaline magmatism associated with this plume event extends to the east as far as Broken Hill (Wingate et al., 1998; Collerson, Report for Impact Minerals). Mineralisation in rocks of this age at Broken Hill, includes the Ni-Co-Cu-Au-PGE systems in ultramafics, nepheline syenites-diorites and gabbros reported by Impact Minerals (ASX Announcements: March 3, 2017; July 11, 2018).

The Paratoo copper - cobalt deposit near Yunta to the east of Burra (Brugger et al., 2006) also contains LREE and HREE secondary mineralisation and is likely to be related to this Neoproterozoic plume event.

8.3 Neoproterozoic Mafic Ultramafic Ni-Cu-Co-PGE Deposits in Rodinia

Rodinia is a late Mesoproterozoic to Neoproterozoic supercontinent that was assembled between 1100–900 Ma (e.g., Ernst et al., 2008, 2016) (Figs.17 and 18). Upwelling of a superplume subsequently resulted in breakup and dispersal of Rodinia between 830 - 720 Ma. Geochronological data from Australia, South China, and the Tarim Craton indicates that breakup occurred between 830 - 800 Ma (Lü et al., 2018). This left a record of plume magmatism with these ages.

A number of Neoproterozoic magmatic Ni–Cu–platinum group element (PGE) sulfide deposits related to this plume magmatism occur in China. Of paramount importance

among these is the giant ~830 Ma Jinchuan deposit (>500 Mt @ 1.2% Ni, 0.7% Cu, Cu/Ni 0.58, ~0.4g/t PGE) which is the largest single magmatic sulphide deposits on Earth (Porter, 2016; Jiao et al. 2018; Mao et al., 2018).

Economic, Ni-Cu-Co-PGE mineralization associated with the Rodinia plume head also occurs in the Lengshuiqing deposit (Yao et al., 2018). Both deposits occur in the continental block that was initially positioned between Australia and Laurentia, directly over the plume head (Figs.17 and 18).

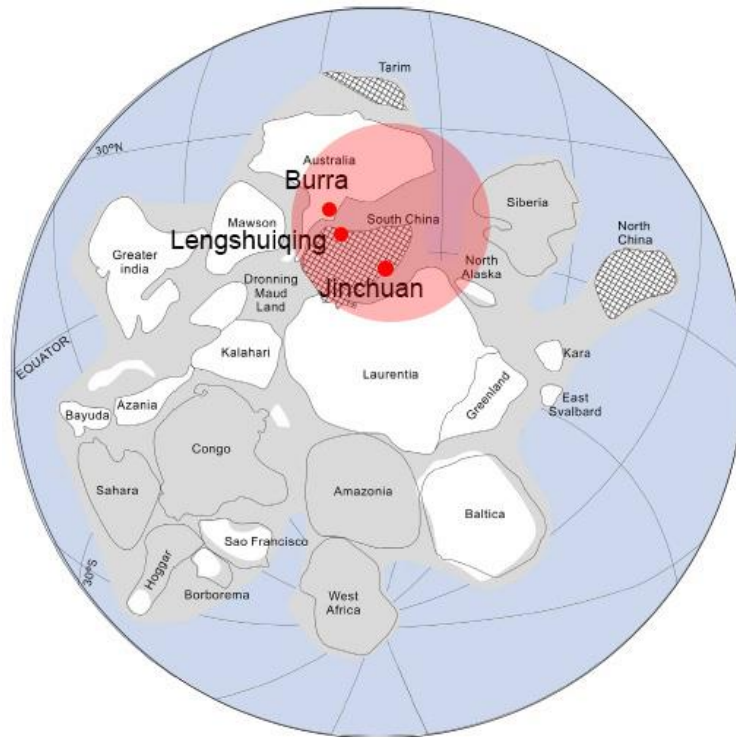


Figure 18: Position of mantle plume head (red circle) responsible for breakup of Rodinia (after Huang et al., 2015), showing the location of Burra in relation to two ~820 Ma mafic-ultramafic intrusions that host Ni-Cu-Co-PGE mineral deposits in China (Porter, 2016; Yao et al., 2018).

In Figure 19, from Niu and Batiza (1997) and Niu et al., (1999), plume-derived magmas that originate in upwellings from the base of the lower mantle retain a record of Earth's primitive (meteoritic) composition and exhibit Ta/U_{PMN} and Nb/Th_{PMN} ratios that plot close to unity. Whereas, magmas contaminated by continental crust, crustal fluids, or fluids derived from subducted slabs, lie in the lower left-hand quadrant (mantle wedge and slab component), with Ta/U_{PMN} of ~0.01 and Nb/Th_{PMN} of ~0.1.

Data for the Jinchuan intrusion shown in Figure 19 clearly confirms the similarity between Jinchuan intrusion in China and the Gairdiner Dykes in South Australia. This provides additional support to for the metallogenic model proposed for Burra.

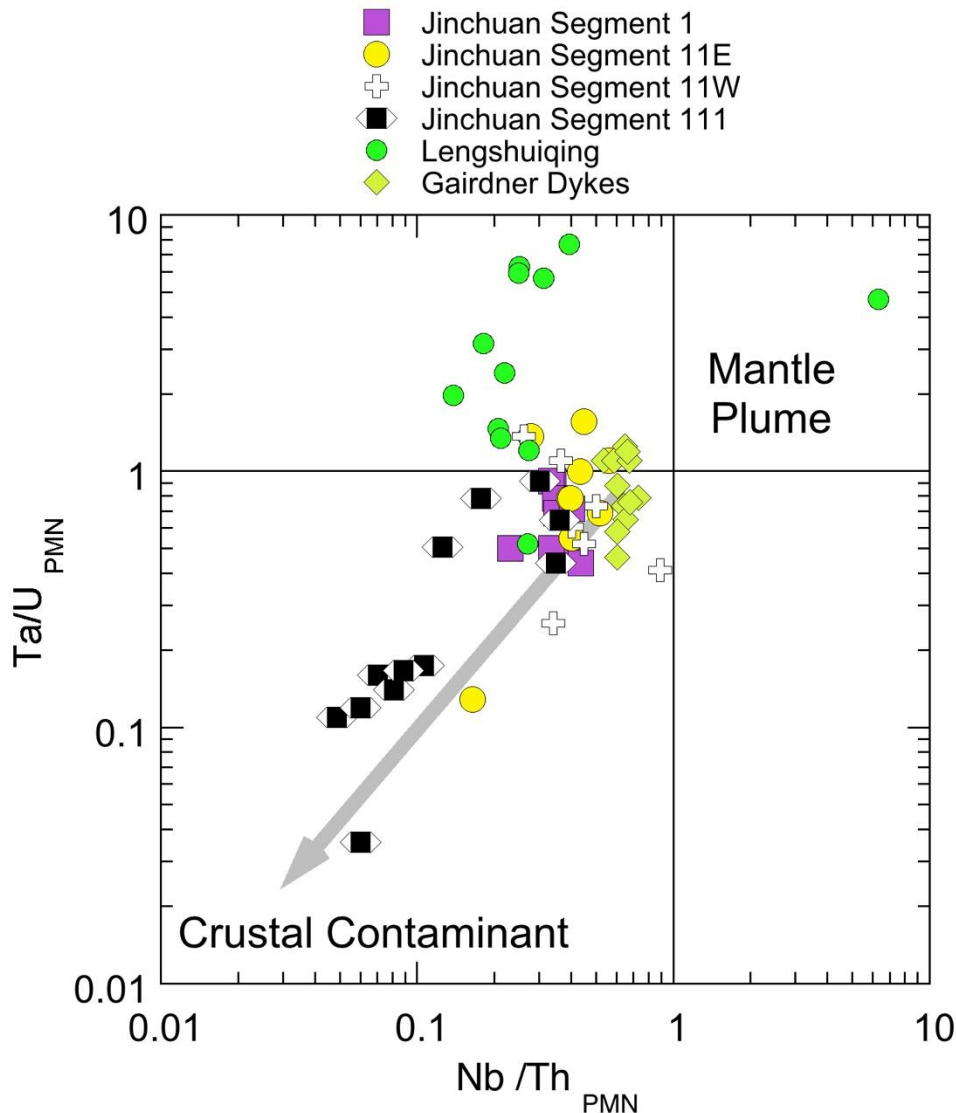


Figure 19: Primitive mantle normalised Ta/U_{PMN} and Nb/Th_{PMN} ratios for Gairdner dykes (Huang et al., 2015) and lithologies from the Jinchuan Intrusion (Mao et al., 2019) [calculated using primitive mantle values from McDonough and Sun (1995) and Lyubetskaya and Korenaga (2007)]. Plume generated suites plot close to Ta/U_{PMN} and Nb/Th_{PMN} values of unity. Some samples from Jinchuan segment 111 show the effect of crustal contamination

8.4 Exploration Implications for the Burra Project

The Rodinia plume model discussed above explains the metal association (Cu-Co-Ni-Au) seen in Ausmex's Burra tenements and thus, has significant exploration implications.

For example, samples from Princess Royal and Willalo exhibit similar ranges in Ni, Cu and Co to lithologies of the Jinchuan intrusion (Figures 20-22). The significant enrichment in Cu, Ni and Co clearly indicates that the Burra mineral systems was derived from an ultramafic to mafic source, that is similar you the host of the Jinchuan deposit.

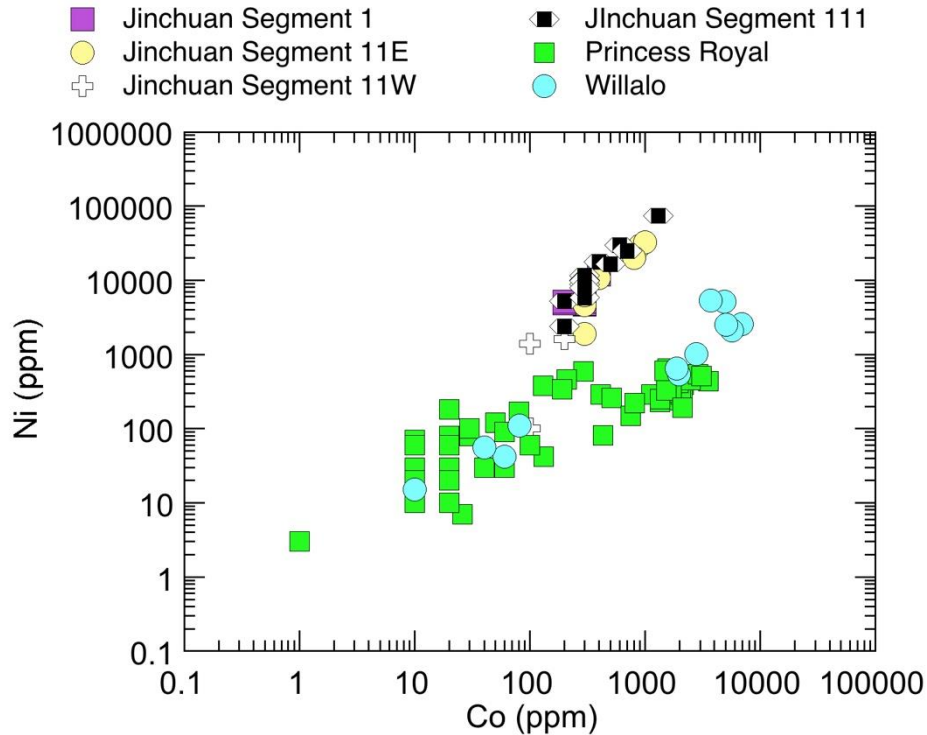


Figure 20: Covariation between Ni and Co in Burra and Jinchuan (Data from Mao et al., 2019). This shows two divergent covariation fractionation trends where some of the Princess Royal sample clearly lie on the Jinchuan trend.

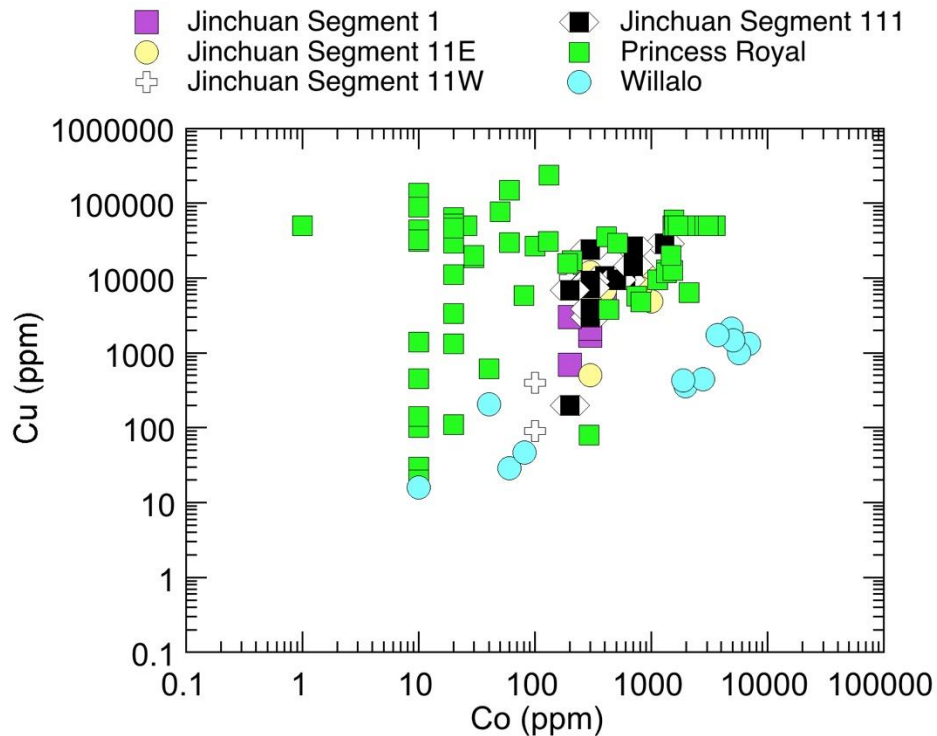


Figure 21: Covariation between Cu and Co in Burra and Jinchuan (Data from Mao et al., 2019). This shows two trends one that is clearly magmatic with systematic covariation between Cu and Co probably in primary sulphides. The other shows significant Cu enrichment in samples with low contents of Co is interpreted to reflect supergene Cu enrichment.

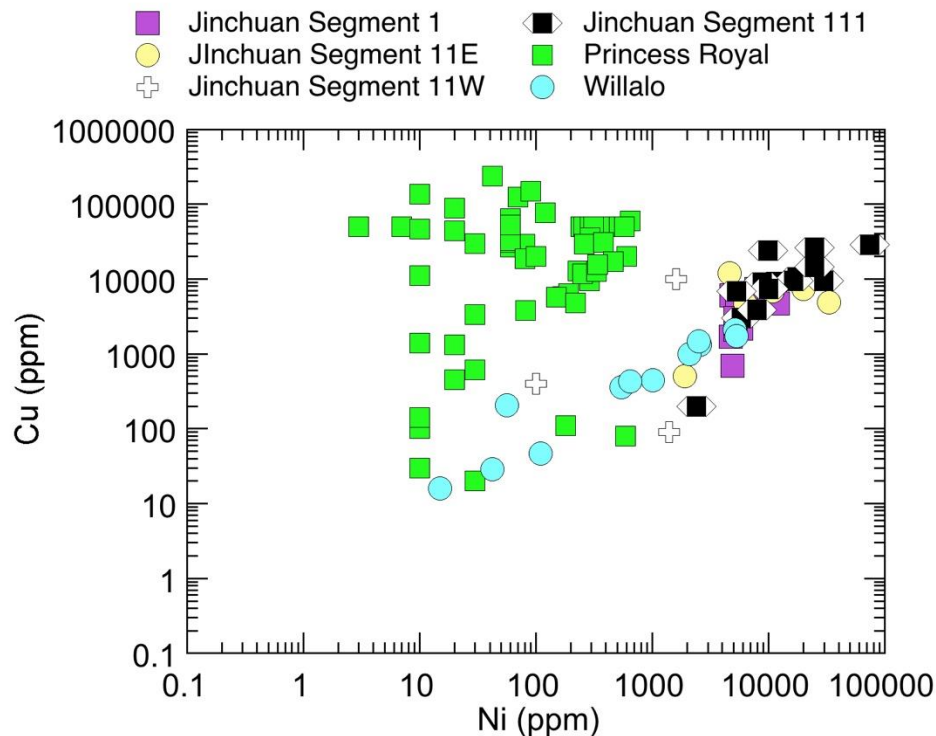


Figure 22: Covariation between Cu and Ni in Burra and Jinchuan (Data from Mao et al., 2019). This shows two trends one that is clearly magmatic with systematic covariation between Cu and Ni probably in primary sulphides. The other shows significant Cu enrichment in samples with low contents of Ni is interpreted to reflect supergene Cu enrichment.

The Burra area is highly prospectivity because of its position in Rodinia relative to the plume head. The terrane lying between the Gawler and Curnamona Cratons is the most proximal region of non-Chinese lithosphere to have experienced plume induced magmatism associated with the breakup of Rodinia at ~820 Ma. This is confirmed by the plume signatures shown by the Gairdner dykes in Figure 19.

The conductive regions seen in the MT and AMT images of the lower-to-middle crust below Burra continue to shallow crustal depths. These conductive zones are interpreted to reflect the presence of a mineral system similar to the Jinchuan mineral deposit in the Burra area.

9. Summary

Key findings related to the nature of the conductive anomalies below Burra are as follows:

- (1) The multiple conductive regions seen in the MT and AMT images of the lower-to-middle crust at Burra, are interpreted as possible sulphide rich domains.
- (2) Metals in the Burra mineral system were derived from an ultramafic plume source
- (3) The Burra mineral system formed between ~800 and 830 Ma during the impact of a lower mantle plume below the late Precambrian supercontinent of Rodinia.
- (4) The Jinchuan deposit in China occurs in another dispersed component of Rodinia.
- (5) The Jinchuan deposit is the largest single magmatic sulphide deposit on Earth with >500 Mt @ 1.2% Ni, 0.7% Cu, Cu/Ni 0.58, ~0.4g/t PGE. It formed during the same plume event.
- (6) Jinchuan mineral system was also feed by multiple magmatic conduits.
- (7) Gairdner mafic dykes and samples from Jinchuan were emplaced during the plume magmatic event and have identical lower mantle normalised Ta/U and Nb/Th ratios of ~ unity. This confirms the lower mantle pedigree of their metal sources.
- (8) Princess Royal samples have non-chondritic Y/Ho and both negative and positive Ce/*Ce anomalies. The non-chondritic Y/Ho ratios indicate that the hydrothermal system was halogen-rich (fluorine-rich).
- (9) The negative and positive Ce/*Ce anomalies indicate that the fluids were oxidising.
- (10) Metals at Burra were transported as F-complexes in halogen-rich fluids and as sulphides in pipe-like conduits.
- (11) They were precipitated when fluids interacted with Neoproterozoic carbonate lithologies.
- (12) Willalo rock chip samples display significant coherent enrichment in Co, Cu and Ni. This is interpreted to indicate proximity to the mafic and ultramafic source of metals in the Burra mineral system.
- (13) The primary metal source for Burra mineral system is inferred to be ~300 Ma older than folding in the region associated with the late Precambrian Delamerian Orogeny.
- (14) Mobilisation of mineralisation during this event is likely to have produced zones of sulphide enrichment.
- (15) This previously unrecognized association Cu-Co-Ni-PGE-Au mineralisation at Burra has a similar source to the giant Jinchuan Deposit in China.
- (16) An othomagmatic ultramafic source explains the association of metals.
- (17) Conductive zones A and B west of Princess Royal are likely targets for a Jinchuan type deposit.

10. Recommendations

This previously unrecognized association Cu-Co-Ni-PGE mineralisation at Burra, that has a similar plume source to the giant Jinchuan Deposit in China, shows the potential for discovery of a new mineral system in SA - possibly Neoproterozoic orthomagmatic or IOCG mineralisation in the southern Flinders Ranges.

To explore this possibility, it is recommended that:

- (1) As these conductive zones continue to shallow depths should be tested by drilling.
- (2) It is recommended that a gravity survey be undertaken to delineate these conductive zones and advance them towards defining one or more drilling targets.
- (3) Willalo rock chip samples have similar mean Cu/Ni ratios to the Jinchuan viz., 0.52 ± 0.12 and 0.53 ± 0.39 respectively. Therefore, Willalo is considered to be a high priority target for Co, Ni, Cu, Au and platinum group elements.
- (4) Samples with high Au contents should be analysed by fire assay for the PGEs, as PGE enrichment is a common feature of alkaline magmas associated with upwelling mantle plumes.

11. References

- Aleinikoff, J.N., Lund, K., Fanning, C.M. (2014) SHRIMP U-Pb and REE data pertaining to the origins of xenotime in Belt Supergroup rocks: evidence for ages of deposition, hydrothermal alteration and metamorphism. *Can. J. Earth Sci.* 52: 722-745.
- AusMex (2018) Additional high-grade cobalt, copper and gold identified at the Burra project. South Australia. ASX Market Release (ASX:AMG) 19th July 2018.
- Bau M., (1996) Controls on the fractionation of isovalent trace elements in magmatic and aqueous systems: Evidence from Y/Ho, Zr/Hf, and lanthanide tetrad effect. *Contrib. Mineral. Petrol.* 123: 323-333.
- Bau, M., Dulski, P., 1995. Comparative study of yttrium and rare-earth element behaviours in fluorine-rich hydrothermal fluids. *Contrib. Mineral. Petrol.* 119, 213-223.
- Betts, P.G., Giles, D., Schaefer, B.F., Mark, G. (2007) 1600–1500 Ma hotspot track in eastern Australia: implications for Mesoproterozoic continental reconstructions. *Terra Nova*, 19: 496-501.
- Betts, P.G., Giles, D., Foden, F., Schaefer, B.F., Mark, G., Pankhurst, M.J., Caroline Forbes, C.J., Williams, H.A., Chalmers, N.C., Hills, Q. (2009) Mesoproterozoic plume-modified orogenesis in eastern Precambrian Australia, *Tectonics* 28: TC3006, doi:10.1029/2008TC002325.
- Brett, P.R., (1956) The geology of an area immediately south of Burra, with particular reference to mineralisation. BSc Hons Thesis School of Earth and Environmental Sciences, Geology & Geophysics, University of Adelaide. <http://hdl.handle.net/2440/84478>
- Brugger, J., Ogierman, J., Pring, A., Waldron, H., and Kolitsch, U. (2006) Origin of the secondary REE-minerals at the Paratoo copper deposit near Yunta, South Australia. *Mineralogical Magazine*, 70: 609-627.
- Brugger, J., Liu, W., Etschmann, B., Mei, Y., Sherman, D.M., Testemale, D.S. (2016) A review of the coordination chemistry of hydrothermal systems, or do coordination changes make ore deposits? *Chemical Geology*, 447: 219-253.
- Buhn, B., (2008) The role of the volatile phase for REE and Y fractionation in low-silica carbonate magmas: implications from natural carbonatites, Namibia. *Mineral. Petrol.* 92: 453-470.
- De Andrade, F.R.D., Möller, P., Dulski, P., 2002. Zr/Hf in carbonatites and alkaline rocks: New data and a re-evaluation. *Revista Brasileira de Geociências*, 3:, 361-370.
- Ernst, R.E., Jowitt, S.M., (2013) Large Igneous Provinces (LIPs) and metallogeny. *Soc. Econ. Geol. Spec. Publ.* 17: 17–51.
- Ernst, R.E., Wingate, M.T.D., Buchan, K.L., Li, Z.X., (2008) Global record of 1600–700 Ma Large Igneous Provinces (LIPs): implications for the reconstruction of the proposed Nuna (Columbia) and Rodinia supercontinents. *Precambrian. Res.* 160: 159–178.
- Haynes, D.W., Cross, K.C., Bills, R.T., and Reed, M.H., (1995) Olympic Dam ore genesis: A fluid-mixing model. *Economic Geology* 90: p. 281–307.
- Heinson, G., Didana, Y., Soeffky, P., Thiel, S. & Wise, T. (2018) The crustal geophysical signature of a world-class magmatic mineral system. *Scientific Reports*, 8: 10608.
- Huang, Q., Kamenetsky, V., McPhie, J., Ehrig, K., Meffre, S., Maas, R., Thompson, J., Kamenetsky, M., Chambefort, I., Apukhtina, O., & Hu, Y. (2015) NeoProterozoic (Ca. 820-830 Ma) mafic dikes at Olympic Dam, South Australia: Links with the Gairdner Large Igneous Province. *Precambrian Res.* 271: 160-172.
- Huang, Q., Kamenetsky, V.S., Ehrig, K., McPhie, J., Kamenetsky, M., Chambefort, I., Apukhtina, O., Chambefort, I., (2017) Effects of hydrothermal alteration on mafic lithologies at the Olympic Dam Cu-U-Au-Ag deposit. *Precambrian Res.* 292: 305-322.

- Jiao, J., Rui, H., Duan, J. (2018) Genesis of the main types of sulphide ore in the Jinchuan Ni–Cu–PGE deposit, NW China: Constraints from texture and mineral chemistry of pyrrhotite. *Geological Journal*. 53:S1, 147-158.
- Johnson, J.P. & Cross, K. (1995) U-Pb geochronological constraints on the genesis of the Olympic Dam Cu-U-Au-Ag deposit, South Australia. *Economic Geology* 90: 1046–1063.
- Johnson, J.P. and McCulloch, M.T. (1995) Sources of mineralising fluids for the Olympic Dam deposit (South Australia): Sm-Nd isotopic constraints. *Chemical Geology* 121: 177-199.
- Landis, G.P. and Hofstra, A.H. (2012) Ore Genesis Constraints on the Idaho Cobalt Belt from Fluid Inclusion Gas, Noble Gas Isotope, and Ion Ratio Analyses. *Economic Geology*, 107: 1189-1205.
- Liu, W., Borg, S.J., Testemale, D., Etschmann, B., Hazemann, J-L., Brugger, J. (2011) Speciation and thermodynamic properties for cobalt chloride complexes in hydrothermal fluids at 35–440°C and 600 bar: An in-situ XAS study. *Geochim. Cosmochim. Acta*, 75: 1227-1248.
- Loubert, M., Bernat, M., Javoy, M., Allegre, C.J. (1972) Rare earth contents in carbonatites. *Earth Planet. Sci. Lett.* 14: 226-232.
- Lü, L-S., Li, H-B., Yang, X-N, Liu, J., Mao, B., Li, B-L. (2018) Neoproterozoic magmatic Ni-Cu-(PGE) sulphide deposits related to the assembly and breakup of the Rodinia supercontinent in China: An overview. *Ore Geology Reviews*, 99: 282-302.
- Lyubetskaya, T., Korenaga, J., (2007) Chemical composition of the Earth's primitive mantle and its variance. *J. Geophys. Res.* 112, B03211, doi:10.1029/2005JB004223.
- Mao, X., Li, L., Liu, Z., Zeng, R., Gick, J.M. Yue, B., Ai, Q. (2019) Multiple magma conduits model of Jinchuan Ni-Cu-(PGE) Deposit, Northwestern China: Constraints from geochemistry of platinum-group elements. *Minerals*, 9: 187; doi: 10.3390/min9030187.
- Mao, Y-J., Barnes, S.J., Duan, J., Qin, K-Z., Godel, B.M. Jiao, J. (2018) Morphology and particle size distribution of olivines and sulphides in the Jinchuan Ni–Cu sulphide deposit: evidence for sulphide percolation in a crystal mush. *J. Petrology* (in press).
- Marks, L., Keiding, J., Wenzel, T., Trumbull, R.B, Veksler, I., Wiedenbeck, W., Markl, G. (2014) F, Cl, and S concentrations in olivine-hosted melt inclusions from mafic dikes in NW Namibia and implications for the environmental impact of the Paraná–Etendeka Large Igneous Province. *Earth Planet Sci Lett.* 392: 39-49.
- McDonough, W. F., Sun S.-S., 1995. The composition of the Earth, *Chem. Geol.*, 120: 223–253
- McPhie, J., Kamenetsky, V. S., Allen, S., Ehrig, K. Agangi, A. & Bath, A. (2011) The fluorine link between a supergiant ore deposit and a silicic large igneous provinces. *Geology*, 39: 1003-1006.
- Niu, Y., Batiza, R. (1997) Trace element evidence from seamounts for recycled oceanic crust in the Eastern Pacific mantle. *Earth Planet. Sci. Lett.* 148: 471-483.
- Niu, Y., Collerson, K.D., Batiza, R., Wendt, I. & Regelous, M. (1999) Origin of enriched-type mid-ocean-ridge basalt at ridges far from mantle plumes: The East Pacific Rise at 11°20'N. *J. Geophys. Res.* 104: 7067-7087.
- Oreskes, N., and Einaudi, M.T., (1990) Origin of rare earth element-enriched hematite breccias at the Olympic Dam Cu-U-Au-Ag deposit, Roxby Downs, South Australia: *Economic Geology*, 85: p. 1–28.
- Porter, T.M. (2016) Regional tectonics, geology, magma chamber processes and mineralisation of the Jinchuan nickel-copper-PGE deposit, Gansu Province, China: A review. *Geoscience Frontiers*, 7: 431-451.

- Preiss, W.V. , Drexel, J.F. , Reid, A.J. (2009) Definition and age of the Koorunga Member of the Skillogalee Dolomite: host for Neoproterozoic (c.790 Ma) porphyry-related copper mineralisation at Burra. *MESA Journal* 55: 19-33.
- Richards, J. P. & Mumin, A. H. (2013) Magmatic-hydrothermal processes within an evolving Earth: Iron oxide-copper-gold and porphyry Cu± Mo± Au deposits. *Geology* 41: 767-770.
- Roberts, D.E., and Hudson, G.R.T., (1983) The Olympic Dam copper-uranium- gold deposit, Roxby Downs, South Australia: *Economic Geology*, 78: 799–822.
- Seward T. M. and Barnes H. L. (1997) Metal transport by hydrothermal ore fluids. In *Geochemistry of Hydrothermal Ore Deposits* (ed. H. L. Barnes). John Wiley & Sons.
- Sheraton, J.W. Sun, S-S., (1997) Mafic dyke swarms of the western Musgrave Block, central Australia: their geochemistry, origin, and relationships to the Giles Complex. *AGSO Journal of Australian Geology and Geophysics*. 16:621-636.
- Slack, J. F. (2006) High REE and Y concentrations in Co-Cu-Au ores of the Blackbird District Idaho. *Economic Geology*, 101: 275-280.
- Wang, X-C., Li, X-H., Li, Z-H., Liu, Y., & Yang, Y-H. (2010) The Willouran basic igneous province of South Australia: Its relationship to the Guibei large igneous province in South China and the breakup of Rodinia. *Lithos*, 119: 569-584.
- Wingate, M.T.D., Campbell, I.H., Compston, W., & Gibson G.M. (1998) Ion microprobe U-Pb ages for Neoproterozoic basaltic magmatism in south-central Australia and implications for breakup of Rodinia. *Precambrian Res.* 87:135-159.
- Yao, J-H., Zhu, W-G., Lai, C., Zhong, H., Bai, Z-J., Ripley, E.M., Li., C. (2018) Petrogenesis and ore genesis of the Lengshuiqing magmatic sulphide deposit in southwest China: Constraints from chalcophile elements (PGE, Se) and Sr-Nd-Os-S isotopes. *Economic Geology*, 113: 675-698.